

# **7 Series FPGAs PCB Design Guide**

**UG483 (v1.13) August 18, 2017**



The information disclosed to you hereunder (the "Materials") is provided solely for the selection and use of Xilinx products. To the maximum extent permitted by applicable law: (1) Materials are made available "AS IS" and with all faults, Xilinx hereby DISCLAIMS ALL WARRANTIES AND CONDITIONS, EXPRESS, IMPLIED, OR STATUTORY, INCLUDING BUT NOT LIMITED TO WARRANTIES OF MERCHANTABILITY, NON-INFRINGEMENT, OR FITNESS FOR ANY PARTICULAR PURPOSE; and (2) Xilinx shall not be liable (whether in contract or tort, including negligence, or under any other theory of liability) for any loss or damage of any kind or nature related to, arising under, or in connection with, the Materials (including your use of the Materials), including for any direct, indirect, special, incidental, or consequential loss or damage (including loss of data, profits, goodwill, or any type of loss or damage suffered as a result of any action brought by a third party) even if such damage or loss was reasonably foreseeable or Xilinx had been advised of the possibility of the same. Xilinx assumes no obligation to correct any errors contained in the Materials, or to advise you of any corrections or update. You may not reproduce, modify, distribute, or publicly display the Materials without prior written consent. Certain products are subject to the terms and conditions of Xilinx's limited warranty, please refer to Xilinx's Terms of Sale which can be viewed at [www.xilinx.com/legal.htm#tos](http://www.xilinx.com/legal.htm#tos); IP cores may be subject to warranty and support terms contained in a license issued to you by Xilinx. Xilinx products are not designed or intended to be fail-safe or for use in any application requiring fail-safe performance; you assume sole risk and liability for use of Xilinx products in such critical applications, please refer to Xilinx's Terms of Sale which can be viewed at [www.xilinx.com/legal.htm#tos](http://www.xilinx.com/legal.htm#tos).

#### **AUTOMOTIVE APPLICATIONS DISCLAIMER**

AUTOMOTIVE PRODUCTS (IDENTIFIED AS "XA" IN THE PART NUMBER) ARE NOT WARRANTED FOR USE IN THE DEPLOYMENT OF AIRBAGS OR FOR USE IN APPLICATIONS THAT AFFECT CONTROL OF A VEHICLE ("SAFETY APPLICATION") UNLESS THERE IS A SAFETY CONCEPT OR REDUNDANCY FEATURE CONSISTENT WITH THE ISO 26262 AUTOMOTIVE SAFETY STANDARD ("SAFETY DESIGN"). CUSTOMER SHALL, PRIOR TO USING OR DISTRIBUTING ANY SYSTEMS THAT INCORPORATE PRODUCTS, THOROUGHLY TEST SUCH SYSTEMS FOR SAFETY PURPOSES. USE OF PRODUCTS IN A SAFETY APPLICATION WITHOUT A SAFETY DESIGN IS FULLY AT THE RISK OF CUSTOMER, SUBJECT ONLY TO APPLICABLE LAWS AND REGULATIONS GOVERNING LIMITATIONS ON PRODUCT LIABILITY.

© Copyright 2011–2017 Xilinx, Inc. Xilinx, the Xilinx logo, Artix, ISE, Kintex, Spartan, Virtex, Vivado, Zynq, and other designated brands included herein are trademarks of Xilinx in the United States and other countries. All other trademarks are the property of their respective owners.

## **Revision History**

The following table shows the revision history for this document.

Date	Version	Revision
03/28/2011	1.0	Initial Xilinx release.
06/22/2011	1.1	Updated <a href="#">Additional Support Resources</a> . Updated <a href="#">Table 2-3</a> and added <a href="#">Table 2-4</a> . Added 680 $\mu$ F to <a href="#">Table 2-5</a> . Updated capacitances in <a href="#">Bulk Capacitor Consolidation Rules</a> . Updated <a href="#">Input Thresholds</a> .
08/16/2011	1.2	Corrected FFG676 and FFG900 packages, and removed SBG324 package from <a href="#">Table 2-3</a> . Added FFG1930 package to <a href="#">Table 2-4</a> . In <a href="#">Figure 5-18</a> title, replaced "TDR" with "Return Loss."
12/15/2011	1.3	Added <a href="#">Table 2-2</a> . Updated <a href="#">Table 2-3</a> and <a href="#">Table 2-4</a> . Updated <a href="#">Example, page 21</a> with Kintex-7 device.
03/19/2012	1.4	Updated <a href="#">Table 2-2</a> and <a href="#">Table 2-4</a> .
10/02/2012	1.5	Added FLG1926, HCG1155, HCG1931, and HCG1932 packages to <a href="#">Table 2-4</a> . In <a href="#">Table 2-5</a> , changed minimum ESR value for 100 $\mu$ F capacitor from 10 m $\Omega$ to 2 m $\Omega$ .

Date	Version	Revision
02/12/2013	1.6	Updated first paragraph of <a href="#">Recommended PCB Capacitors per Device</a> . Added <a href="#">Fixed Package Capacitors per Device</a> . In <a href="#">Table 2-2</a> , removed XC7A350T and added XC7A200T (SBG484). In <a href="#">Table 2-4</a> , removed XC7V1500T and corrected packages for XC7VX1140T from FFG to FLG. Added note about Pb-free packages to <a href="#">Table 2-2</a> , <a href="#">Table 2-3</a> , and <a href="#">Table 2-4</a> . In <a href="#">Table 2-5</a> , updated 680 $\mu$ F, 47 $\mu$ F, and 4.7 $\mu$ F rows, and added second 330 $\mu$ F row. Added <a href="#">Table 2-6</a> to <a href="#">Table 2-9</a> . Updated second paragraph of <a href="#">PCB Bulk Capacitors</a> , page 23. Updated <a href="#">PCB Capacitor Placement and Mounting Techniques</a> .
06/13/2013	1.7	Added RF676 and RF900 packages to <a href="#">Table 2-3</a> . Added RF1157, RF1761, and RF1930 packages to <a href="#">Table 2-4</a> . In <a href="#">Table 2-5</a> , updated 680 $\mu$ F, 100 $\mu$ F, 47 $\mu$ F, and 4.7 $\mu$ F rows. Added RF676 and RF900 packages to <a href="#">Table 2-6</a> . Added RF1157, RF1761, and RF1930 packages to <a href="#">Table 2-8</a> . Added capacitor V to <a href="#">PCB Bulk Capacitors</a> , page 23 and <a href="#">PCB Bulk Capacitors</a> , page 24. In <a href="#">0402 Ceramic Capacitors</a> , replaced 0805 ceramic capacitor with 0402. Updated <a href="#">Figure 2-1</a> . In <a href="#">Figure 2-6</a> , replaced 0805 capacitor with 0402.
09/13/2013	1.8	Added Artix-7 devices XC7A35T, XC7A50T, and XC7A75T to and updated <a href="#">Table 2-2</a> . Removed this note: <i>All packages listed are Pb-free. Some packages are available in Pb option</i> from <a href="#">Table 2-3</a> , <a href="#">Table 2-6</a> , and <a href="#">Table 2-8</a> . Removed Note 4 from <a href="#">Table 2-4</a> .
05/13/2014	1.9	In <a href="#">Recommended PCB Capacitors per Device</a> , added reference to <a href="#">XMP277</a> , 7 Series Schematic Review Recommendations. In <a href="#">Table 2-2</a> , corrected V <sub>CCO</sub> Bank 0 capacitance from 4.7 $\mu$ F to 47 $\mu$ F; added 100 $\mu$ F to V <sub>CCO</sub> all other Banks column; added CPG236, CSG325, RB484, RS484, and RB676 packages; added XA7A35T, XA7A50T, XA7A75T, XA7A100T, XQ7A50T, XQ7A100T, and XQ7A200T devices; and updated Note 3. Added this note: “Decoupling capacitors cover down to approximately 100 KHz” to <a href="#">Table 2-2</a> , <a href="#">Table 2-3</a> , and <a href="#">Table 2-4</a> . Added 47 $\mu$ F to V <sub>CCO</sub> all other Banks column in <a href="#">Table 2-3</a> and <a href="#">Table 2-4</a> . In <a href="#">Table 2-4</a> , added FLG1155 and FLG1931 packages for XC7VH580T, removed HCG1932 package for XC7VH580T, removed HCG1931 package for XC7VH870T, and added FLG1932 package for XC7VH870T. Updated <a href="#">Table 2-5</a> , including the addition of 0.47 $\mu$ F. In <a href="#">Table 2-8</a> , added FLG1155 and FLG1931 packages for XC7VH580T, removed HCG1931 package for XC7VH870T, removed HCG1932 package for XC7VH580T, and added FLG1932 package for XC7VH870T. Updated list of bulk capacitors in <a href="#">PCB Bulk Capacitors</a> , page 23 and added note. Replaced 0402 with 0805 package in <a href="#">PCB High-Frequency Capacitors</a> . Removed Example section from <a href="#">Bulk Capacitor Consolidation Rules</a> . Updated list of bulk capacitors in <a href="#">PCB Bulk Capacitors</a> , page 24. In <a href="#">0805 and 0603 Ceramic Capacitors</a> , replaced 0402 with 0805 and 0603 capacitors. Removed 0402 from <a href="#">Figure 2-1</a> . Updated first paragraph of <a href="#">Noise Limits</a> . Added V <sub>CCAUX_IO</sub> to <a href="#">Power Supply Consolidation</a> . Updated last paragraph of <a href="#">Unconnected V<sub>CCO</sub> Pins</a> . Updated paragraph after <a href="#">Figure 2-9</a> .
11/12/2014	1.10	Removed “pin planning” from document title. Added reference to 7 Series FPGAs Packaging and Pinout Product Specification User Guide in <a href="#">Lands</a> . Added XC7A15T and XA7A15T devices to <a href="#">Table 2-2</a> . Added note about 47 $\mu$ F capacitor being required for V <sub>CCO</sub> banks to <a href="#">Table 2-3</a> and <a href="#">Table 2-4</a> and updated the same to note 3 in <a href="#">Table 2-2</a> . Removed V <sub>RIPPLE</sub> from <a href="#">Noise Limits</a> .
04/07/2016	1.11	Added FBV484, FBV676, and FFFV1156 packages to <a href="#">Table 2-2</a> and deleted Note 4 ( <i>All packages listed are Pb-free. Some packages are available in Pb option</i> ). Added FBV484, FBV676, FFFV676, FBV900, FFFV900, FFFV901, and FFFV1156 packages to <a href="#">Table 2-3</a> . Added FFFV1157, FFFV1158, RF1158, FFG1761, and FFFV1927 packages to <a href="#">Table 2-4</a> . Added FBV484, FBV676, FFFV676, FBV900, FFFV900, FFFV901, and FFFV1156 packages to <a href="#">Table 2-6</a> . Added FFFV1157, FFFV1158, RF1158, FFFV1761, and FFFV1927 packages and device XQ7VX690T to <a href="#">Table 2-6</a> . Added FFFV1157, FFFV1158, RF1158, FFFV1761, and FFFV1927 packages to <a href="#">Table 2-8</a> .

Date	Version	Revision
01/10/2017	1.12	Updated introductory paragraph in <a href="#">About This Guide</a> . Changed “100 MHz” to “10 MHz” in third paragraph, updated fourth paragraph, and added “GTP” and UG482 reference in last paragraph under <a href="#">Recommended PCB Capacitors per Device</a> . Added <a href="#">Table 2-1</a> for Spartan-7 devices. Added XC7A12T and XC7A25T devices to <a href="#">Table 2-2</a> .
08/18/2017	1.13	<p>In <a href="#">Table 2-1</a>:</p> <ul style="list-style-type: none"> <li>• Added FTGB196 package for XC7S6, XC7S15, XC7S25, and XC7S50 devices.</li> <li>• Added FGGA676 package for XC7S75 device.</li> <li>• Removed V<sub>CCINT</sub> columns at 680 µF and 47 µF.</li> <li>• Removed V<sub>CCO</sub> bank 0 column.</li> <li>• Removed note 5.</li> </ul> <p>In <a href="#">Table 2-2</a>, replaced CPG236 with CPG238 package for XC7A12T and XC7A25T devices, and added capacitance values for CSG325 package in XC7A12T and XC7A25T devices. Removed HCG1155, HCG1931, and HCG1931 packages from <a href="#">Table 2-4</a> and <a href="#">Table 2-8</a> per the customer notice <a href="#">XCN14005</a>, <i>Product Discontinuation Notice For Virtex-7 HT FPGA HCG Packages</i>. In <a href="#">Table 2-11</a>, replaced Agilent and Sigrity vendors with Cadence.</p>

# Table of Contents

---

Revision History .....	2
<b>Preface: About This Guide</b>	
Guide Contents .....	7
Additional Support Resources .....	7
<b>Chapter 1: PCB Technology Basics</b>	
PCB Structures .....	9
Traces .....	9
Planes .....	9
Vias .....	10
Pads and Antipads .....	10
Lands .....	10
Dimensions .....	10
Transmission Lines .....	11
Return Currents .....	12
<b>Chapter 2: Power Distribution System</b>	
PCB Decoupling Capacitors .....	13
Recommended PCB Capacitors per Device .....	13
Fixed Package Capacitors per Device .....	14
Capacitor Specifications .....	19
Bulk Capacitor Consolidation Rules .....	24
PCB Capacitor Placement and Mounting Techniques .....	24
Basic PDS Principles .....	25
Noise Limits .....	25
Role of Inductance .....	27
Capacitor Parasitic Inductance .....	27
PCB Current Path Inductance .....	29
Plane Inductance .....	30
Capacitor Effective Frequency .....	33
Capacitor Anti-Resonance .....	34
Capacitor Placement Background .....	35
V <sub>REF</sub> Stabilization Capacitors .....	36
Power Supply Consolidation .....	36
Unconnected V <sub>CCO</sub> Pins .....	36
Simulation Methods .....	36
PDS Measurements .....	38
Noise Magnitude Measurement .....	38
Noise Spectrum Measurements .....	40
Optimum Decoupling Network Design .....	42
Troubleshooting .....	42
Possibility 1: Excessive Noise from Other Devices on the PCB .....	42
Possibility 2: Parasitic Inductance of Planes, Vias, or Connecting Traces .....	42

Possibility 3: I/O Signals in PCB are Stronger Than Necessary . . . . .	43
Possibility 4: I/O Signal Return Current Traveling in Sub-Optimal Paths . . . . .	43

## Chapter 3: SelectIO Signaling

<b>Interface Types.</b> . . . . .	45
Single-Ended versus Differential Interfaces . . . . .	45
SDR versus DDR Interfaces . . . . .	46
<b>Single-Ended Signaling</b> . . . . .	46
Modes and Attributes . . . . .	46
Input Thresholds . . . . .	46
Topographies and Termination . . . . .	47

## Chapter 4: PCB Materials and Traces

<b>How Fast is Fast?</b> . . . . .	57
<b>Dielectric Losses</b> . . . . .	57
Relative Permittivity . . . . .	57
Loss Tangent . . . . .	58
Skin Effect and Resistive Losses . . . . .	58
Choosing the Substrate Material . . . . .	58
<b>Traces.</b> . . . . .	59
Trace Geometry . . . . .	59
Trace Characteristic Impedance Design for High-Speed Transceivers . . . . .	59
Trace Routing . . . . .	61
Plane Splits . . . . .	61
Return Currents . . . . .	61
Simulating Lossy Transmission Lines . . . . .	62
<b>Cable</b> . . . . .	62
Connectors . . . . .	62
Skew Between Conductors . . . . .	62

## Chapter 5: Design of Transitions for High-Speed Signals

<b>Excess Capacitance and Inductance</b> . . . . .	63
<b>Time Domain Reflectometry</b> . . . . .	63
<b>BGA Package</b> . . . . .	65
<b>SMT Pads</b> . . . . .	65
<b>Differential Vias</b> . . . . .	70
<b>P/N Crossover Vias.</b> . . . . .	73
<b>SMA Connectors</b> . . . . .	73
<b>Backplane Connectors.</b> . . . . .	73
<b>Microstrip/Stripline Bends</b> . . . . .	73

# About This Guide

---

Xilinx® 7 series FPGAs include four FPGA families that are all designed for lowest power to enable a common design to scale across families for optimal power, performance, and cost. The Spartan®-7 family is the lowest density with the lowest cost entry point into the 7 series portfolio. The Artix®-7 family is optimized for highest performance-per-watt and bandwidth-per-watt for cost-sensitive, high volume applications. The Kintex®-7 family is an innovative class of FPGAs optimized for the best price-performance. The Virtex®-7 family is optimized for highest system performance and capacity.

This guide provides information on PCB design for 7 series FPGAs, with a focus on strategies for making design decisions at the PCB and interface level. This 7 series FPGAs PCB design user guide is part of an overall set of documentation on the 7 series FPGAs, which is available on the Xilinx website at [www.xilinx.com/documentation](http://www.xilinx.com/documentation).

## Guide Contents

This guide contains the following chapters:

- [Chapter 1, PCB Technology Basics](#), discusses the basics of current PCB technology focusing on physical structures and common assumptions.
- [Chapter 2, Power Distribution System](#), covers the power distribution system for 7 series FPGAs, including all details of decoupling capacitor selection, use of voltage regulators and PCB geometries, simulation and measurement.
- [Chapter 3, SelectIO Signaling](#), contains information on the choice of SelectIO™ standards, I/O topographies, and termination strategies as well as information on simulation and measurement techniques.
- [Chapter 4, PCB Materials and Traces](#), provides some guidelines on managing signal attenuation to obtain optimal performance for high-frequency applications.
- [Chapter 5, Design of Transitions for High-Speed Signals](#), addresses the interface at either end of a transmission line. The provided analyses and examples can greatly accelerate the specific design.

## Additional Support Resources

To find additional documentation, see the Xilinx support website at:

<http://www.xilinx.com/support>.





## PCB Technology Basics

---

Printed circuit boards (PCBs) are electrical systems, with electrical properties as complicated as the discrete components and devices mounted to them. The PCB designer has complete control over many aspects of the PCB; however, current technology places constraints and limits on the geometries and resulting electrical properties. The following information is provided as a guide to the freedoms, limitations, and techniques for PCB designs using FPGAs.

This chapter contains the following sections:

- [PCB Structures](#)
- [Transmission Lines](#)
- [Return Currents](#)

### PCB Structures

PCB technology has not changed significantly in the last few decades. An insulator substrate material (usually FR4, an epoxy/glass composite) with copper plating on both sides has portions of copper etched away to form conductive paths. Layers of plated and etched substrates are glued together in a stack with additional insulator substrates between the etched substrates. Holes are drilled through the stack. Conductive plating is applied to these holes, selectively forming conductive connections between the etched copper of different layers.

While there are advancements in PCB technology, such as material properties, the number of stacked layers used, geometries, and drilling techniques (allowing holes that penetrate only a portion of the stackup), the basic structures of PCBs have not changed. The structures formed through the PCB technology are abstracted to a set of physical/electrical structures: traces, planes (or planelets), vias, and pads.

#### Traces

A trace is a physical strip of metal (usually copper) making an electrical connection between two or more points on an X-Y coordinate of a PCB. The trace carries signals between these points.

#### Planes

A plane is an uninterrupted area of metal covering the entire PCB layer. A planelet, a variation of a plane, is an uninterrupted area of metal covering only a portion of a PCB layer. Typically, a number of planelets exist in one PCB layer. Planes and planelets distribute power to a number of points on a PCB. They are very important in the

transmission of signals along traces because they are the return current transmission medium.

## Vias

A via is a piece of metal making an electrical connection between two or more points in the Z space of a PCB. Vias carry signals or power between layers of a PCB. In current plated-through-hole (PTH) technology, a via is formed by plating the inner surface of a hole drilled through the PCB. In current microvia technology (also known as High Density Interconnect or HDI), a via is formed with a laser by ablating the substrate material and deforming the conductive plating. These microvias cannot penetrate more than one or two layers, however, they can be stacked or stair-stepped to form vias traversing the full board thickness.

## Pads and Antipads

Because PTH vias are conductive over the whole length of the via, a method is needed to selectively make electrical connections to traces, planes, and planelets of the various layers of a PCB. This is the function of pads and antipads.

Pads are small areas of copper in prescribed shapes. Antipads are small areas in prescribed shapes where copper is removed. Pads are used both with vias and as exposed outer-layer copper for mounting of surface-mount components. Antipads are used mainly with vias.

For traces, pads are used to make the electrical connection between the via and the trace or plane shape on a given layer. For a via to make a solid connection to a trace on a PCB layer, a pad must be present for mechanical stability. The size of the pad must meet drill tolerance/registration restrictions.

Antipads are used in planes. Because plane and planelet copper is otherwise uninterrupted, any via traveling through the copper makes an electrical connection to it. Where vias are not intended to make an electrical connection to the planes or planelets passed through, an antipad removes copper in the area of the layer where the via penetrates.

## Lands

For the purposes of soldering surface mount components, pads on outer layers are typically referred to as lands or solder lands. Making electrical connections to these lands usually requires vias. Due to manufacturing constraints of PTH technology, it is rarely possible to place a via inside the area of the land. Instead, this technology uses a short section of trace connecting to a surface pad. The minimum length of the connecting trace is determined by minimum dimension specifications from the PCB manufacturer. Microvia technology is not constrained, and vias can be placed directly in the area of a solder land. For further information regarding PCB lands and BGA packages, refer to the “Recommended PCB Design Rules for BGA Packages” appendix of *7 Series FPGAs Packaging and Pinout Product Specification User Guide* ([UG475](#)).

## Dimensions

The major factors defining the dimensions of the PCB are PCB manufacturing limits, FPGA package geometries, and system compliance. Other factors such as Design For Manufacturing (DFM) and reliability impose further limits, but because these are application specific, they are not documented in this user guide.

The dimensions of the FPGA package, in combination with PCB manufacturing limits, define most of the geometric aspects of the PCB structures described in this section ([PCB Structures](#)), both directly and indirectly. This significantly constrains the PCB designer. The package ball pitch (1.0 mm for FF packages) defines the land pad layout. The minimum surface feature sizes of current PCB technology define the via arrangement in the area under the device. Minimum via diameters and *keep-out areas* around those vias are defined by the PCB manufacturer. These diameters limit the amount of space available in-between vias for routing of signals in and out of the via array underneath the device. These diameters define the maximum trace width in these *breakout* traces. PCB manufacturing limits constrain the minimum trace width and minimum spacing.

The total number of PCB layers necessary to accommodate an FPGA is defined by the number of signal layers and the number of plane layers.

- The number of signal layers is defined by the number of I/O signal traces routed in and out of an FPGA package (usually following the total User I/O count of the package).
- The number of plane layers is defined by the number of power and ground plane layers necessary to bring power to the FPGA and to provide references and isolation for signal layers.

Most PCBs for large FPGAs range from 12 to 22 layers.

System compliance often defines the total thickness of the board. Along with the number of board layers, this defines the maximum layer thickness, and therefore, the spacing in the Z direction of signal and plane layers to other signal and plane layers. Z-direction spacing of signal trace layers to other signal trace layers affects crosstalk. Z-direction spacing of signal trace layers to reference plane layers affects signal trace impedance. Z-direction spacing of plane layers to other plane layers affects power system parasitic inductance.

Z-direction spacing of signal trace layers to reference plane layers (defined by total board thickness and number of board layers) is a defining factor in trace impedance. Trace width (defined by FPGA package ball pitch and PCB via manufacturing constraints) is another factor in trace impedance. A designer often has little control over trace impedance in area of the via array beneath the FPGA. When traces escape the via array, their width can change to the width of the target impedance (usually 50Ω single-ended).

Decoupling capacitor placement and discrete termination resistor placement are other areas of trade-off optimization. DFM constraints often define a keep-out area around the perimeter of the FPGA (device footprint) where no discrete components can be placed. The purpose of the keep-out area is to allow room for assembly and rework where necessary. For this reason, the area just outside the keep-out area is one where components compete for placement. It is up to the PCB designer to determine the high priority components. Decoupling capacitor placement constraints are described in [Chapter 2, Power Distribution System](#). Termination resistor placement constraints must be determined through signal integrity simulation, using IBIS or SPICE.

## Transmission Lines

The combination of a signal trace and a reference plane forms a transmission line. All I/O signals in a PCB system travel through transmission lines.

For single-ended I/O interfaces, both the signal trace and the reference plane are necessary to transmit a signal from one place to another on the PCB. For differential I/O interfaces, the transmission line is formed by the combination of two traces and a reference plane.

While the presence of a reference plane is not strictly necessary in the case of differential signals, it is necessary for practical implementation of differential traces in PCBs.

Good signal integrity in a PCB system is dependent on having transmission lines with controlled impedance. Impedance is determined by the geometry of the traces and the dielectric constant of the material in the space around the signal trace and between the signal trace and the reference plane.

The dielectric constant of the material in the vicinity of the trace and reference plane is a property of the PCB laminate materials, and in the case of surface traces, a property of the air or fluid surrounding the board. PCB laminate is typically a variant of FR4, though it can also be an exotic material.

While the dielectric constant of the laminate varies from board to board, it is fairly constant within one board. Therefore, the relative impedance of transmission lines in a PCB is defined most strongly by the trace geometries and tolerances. Impedance variance can occur based on the presence or absence of glass in a local portion of the laminate weave, but this rarely poses issues except in high-speed (>6 Gb/s) interfaces.

## Return Currents

An often neglected aspect of transmission lines and their signal integrity is return current. It is incorrect to assume that a signal trace by itself forms a transmission line. Currents flowing in a signal trace have an equal and opposite complimentary current flowing in the reference plane beneath them. The relationship of the trace voltage and trace current to reference plane voltage and reference plane current defines the characteristic impedance of the transmission line formed by the trace and reference plane. While interruption of reference plane continuity beneath a trace is not as dramatic in effect as severing the signal trace, the performance of the transmission line and any devices sharing the reference plane is affected.

It is important to pay attention to reference plane continuity and return current paths. Interruptions of reference plane continuity, such as holes, slots, or isolation splits, cause significant impedance discontinuities in the signal traces. They can also be a significant source of crosstalk and contributor to Power Distribution System (PDS) noise. The importance of return current paths cannot be underestimated.

## Power Distribution System

---

This chapter documents the power distribution system (PDS) for 7 series FPGAs, including decoupling capacitor selection, placement, and PCB geometries. A simple decoupling method is provided for each 7 series FPGA. Basic PDS design principles are covered, as well as simulation and analysis methods. This chapter contains the following sections:

- [PCB Decoupling Capacitors](#)
- [Basic PDS Principles](#)
- [Simulation Methods](#)
- [PDS Measurements](#)
- [Troubleshooting](#)

### PCB Decoupling Capacitors

#### Recommended PCB Capacitors per Device

A simple PCB-decoupling network for the Spartan®-7 devices is listed in [Table 2-1](#), for the Artix™-7 devices in [Table 2-2](#), for the Kintex™-7 devices in [Table 2-3](#), and for the Virtex®-7 devices in [Table 2-4](#).

In [Table 2-1](#), [Table 2-2](#), [Table 2-3](#), and [Table 2-4](#), the optimized quantities of PCB decoupling capacitors assume that the voltage regulators have stable output voltages and meet the regulator manufacturer's minimum output capacitance requirements.

Decoupling methods other than those presented in these tables can be used, but the decoupling network should be designed to meet or exceed the performance of the simple decoupling networks presented here. The impedance of the alternate network must be less than or equal to that of the recommended network across frequencies from 100 KHz to 10 MHz.

Because device capacitance requirements vary with CLB and I/O utilization, PCB decoupling guidelines are provided on a per-device basis based on very high utilization so as to cover a majority of use cases. Resource usage consists (in part) of:

- 80% of LUTs and registers at 245 MHz
- 80% block RAM and DSP at 491 MHz
- 50% MMCM and 25% PLL at 500 MHz
- 100% I/O at SSTL 1.2/1.35 at 1,200/800 MHz

The Xilinx Power Estimator (XPE) tool is used to estimate the current on each power rail. [DS189](#), *Spartan 7 FPGAs Data Sheet: DC and AC Switching Characteristics*, [DS181](#), *Artix 7*

FPGAs Data Sheet: DC and AC Switching Characteristics, [DS182](#), Kintex 7 FPGAs Data Sheet: DC and AC Switching Characteristics, and [DS183](#), Virtex 7 FPGAs Data Sheet: DC and AC Switching Characteristics provide the operating range for all of the various power rails. The PCB designer should ensure that the AC ripple plus the DC tolerance of the voltage regulator do not exceed the operating range.

The capacitor numbers shown in this user guide are based on the following assumptions:

$V_{CCINT}$  operating range from the data sheet = 3%;

Assumed DC tolerance = 1%;

Therefore, allowable AC ripple = 3% – 1% = 2%.

The target impedance is calculated using the 2% AC ripple along with the current estimates from XPE for the above resource utilization to arrive at the capacitor recommendations.

$V_{CCINT}$ ,  $V_{CCAUX}$ , and  $V_{CCBRAM}$  capacitors are listed as the quantity per device, while  $V_{CCO}$  capacitors are listed as the quantity per I/O bank. Device performance at full utilization is equivalent across all devices when using these recommended networks.

[Table 2-1](#), [Table 2-2](#), [Table 2-3](#), and [Table 2-4](#) do not provide the decoupling networks required for the GTP, GTX or GTH transceiver power supplies. For this information, refer to [UG482](#), 7 Series FPGAs GTP Transceivers User Guide or [UG476](#), 7 Series FPGAs GTX/GTH Transceivers User Guide. For a comprehensive schematic review checklist that complements this user guide, refer to [XMP277](#), 7 Series Schematic Review Recommendations.

## Fixed Package Capacitors per Device

Some 7 series devices require fewer PCB capacitors because high-frequency ceramic capacitors are already present inside the device package (mounted on the package substrate). [Table 2-6](#) and [Table 2-8](#) list the package capacitors for Kintex-7 and Virtex-7 devices. Spartan-7 and **Artix-7 devices do not have package capacitors.**

## Required PCB Capacitor Quantities

[Table 2-1](#) lists the PCB decoupling capacitor guidelines per  $V_{CC}$  supply rail for Spartan-7 devices.

**Table 2-1: Required PCB Capacitor Quantities per Device: Spartan-7 Devices<sup>(1)(2)</sup>**

Package	Device	$V_{CCINT}$				$V_{CCBRAM}$				$V_{CCAUX}$			$V_{CCO}$ (per Bank)		
		330 $\mu$ F	100 $\mu$ F	4.7 $\mu$ F	0.47 $\mu$ F	100 $\mu$ F	47 $\mu$ F	4.7 $\mu$ F	0.47 $\mu$ F	47 $\mu$ F	4.7 $\mu$ F	0.47 $\mu$ F	47 $\mu$ F or 100 $\mu$ F <sup>(3)</sup>	4.7 $\mu$ F	0.47 $\mu$ F
CPGA196	XC7S6	0	1	1	1	0	1	1	1	1	1	2	1	2	4
CSGA225	XC7S6	0	1	1	1	0	1	1	1	1	1	2	1	2	4
FTGB196	XC7S6	0	1	1	1	0	1	1	1	1	1	2	1	2	4
CPGA196	XC7S15	0	1	2	2	0	1	1	1	1	1	2	1	2	4
CSGA225	XC7S15	0	1	2	2	0	1	1	1	1	1	2	1	2	4
FTGB196	XC7S15	0	1	2	2	0	1	1	1	1	1	2	1	2	4
CSGA225	XC7S25	0	1	2	3	0	1	1	1	1	1	2	1	2	4
CSGA324	XC7S25	0	1	2	3	0	1	1	1	1	1	2	1	2	4
FTGB196	XC7S25	0	1	2	3	0	1	1	1	1	1	2	1	2	4

**Table 2-1: Required PCB Capacitor Quantities per Device: Spartan-7 Devices<sup>(1)(2)</sup> (Continued)**

Package	Device	V <sub>CCINT</sub>				V <sub>CCBRAM</sub>				V <sub>CCAUX</sub>			V <sub>CCO</sub> (per Bank)		
		330 µF	100 µF	4.7 µF	0.47 µF	100 µF	47 µF	4.7 µF	0.47 µF	47 µF	4.7 µF	0.47 µF	47 µF or 100 µF <sup>(3)</sup>	4.7 µF	0.47 µF
CSGA324	XC7S50	0	1	3	5	1	1	1	1	1	2	3	1	2	4
FTGB196	XC7S50	0	1	3	5	1	1	1	1	1	1	3	1	2	4
FGGA484	XC7S50	0	1	3	5	1	1	1	1	1	2	4	1	2	4
FGGA484	XC7S75	0	1	4	7	1	1	1	1	1	3	7	1	2	4
FGGA676	XC7S75	0	1	4	7	1	1	1	1	1	3	7	1	2	4
FGGA484	XC7S100	0	1	5	8	1	1	1	1	1	3	7	1	2	4
FGGA676	XC7S100	0	1	5	8	1	1	1	1	1	3	7	1	2	4

**Notes:**

1. PCB capacitor specifications are listed in Table 2-5.
2. Total includes all capacitors for all supplies. The values in this table account for the number of I/O banks in the device.
3. One 47 µF (or 100 µF) capacitor is required for up to four V<sub>CCO</sub> banks when powered by the same voltage.
4. Decoupling capacitors cover down to approximately 100 KHz.

Table 2-2 lists the PCB decoupling capacitor guidelines per V<sub>CC</sub> supply rail for Artix-7 devices.

**Table 2-2: Required PCB Capacitor Quantities per Device: Artix-7 Devices<sup>(1)(2)</sup>**

Package	Device	V <sub>CCINT</sub>						V <sub>CCBRAM</sub>				V <sub>CCAUX</sub>			V <sub>CCO</sub> Bank 0	V <sub>CCO</sub> all other Banks (per Bank)		
		680 µF	330 µF	100 µF	47 µF	4.7 µF	0.47 µF	100 µF	47 µF	4.7 µF	0.47 µF	47 µF	4.7 µF	0.47 µF	47 µF	47 µF or 100 µF <sup>(3)</sup>	4.7 µF	0.47 µF
CPG238	XC7A12T	0	0	1	0	1	2	0	1	0	1	1	1	2	1	1	2	4
CSG325	XC7A12T	0	0	1	0	1	2	0	1	0	1	1	1	2	1	1	2	4
CPG236	XC7A15T XA7A15T	0	0	1	0	2	2	0	1	0	1	1	1	2	1	1	2	4
CPG238	XC7A25T	0	0	1	0	2	3	0	1	0	1	1	1	2	1	1	2	4
CSG325	XC7A25T	0	0	1	0	2	3	0	1	0	1	1	1	2	1	1	2	4
CPG236	XC7A35T XA7A35T	0	0	1	0	2	3	0	1	0	1	1	1	2	1	1	2	4
CPG236	XC7A50T XA7A50T	0	1	0	0	3	5	1	0	0	1	1	1	2	1	1	2	4
FTG256	XC7A15T	0	0	1	0	2	2	0	1	0	1	1	2	3	1	1	2	4
FTG256	XC7A35T	0	0	1	0	2	3	0	1	0	1	1	2	3	1	1	2	4
FTG256	XC7A50T	0	1	0	0	3	5	1	0	0	1	1	2	3	1	1	2	4
FTG256	XC7A75T	0	1	0	0	4	6	1	0	0	2	1	2	3	1	1	2	4
FTG256	XC7A100T	0	1	0	0	6	8	1	0	0	2	1	2	3	1	1	2	4
CSG324	XC7A15T XA7A15T	0	0	1	0	2	2	0	1	0	1	1	2	4	1	1	2	4
CSG324	XC7A35T XA7A35T	0	0	1	0	2	3	0	1	0	1	1	2	4	1	1	2	4
CSG324	XC7A50T XA7A50T	0	1	0	0	3	5	1	0	0	1	1	2	4	1	1	2	4

Table 2-2: Required PCB Capacitor Quantities per Device: Artix-7 Devices<sup>(1)(2)</sup> (Continued)

Package	Device	V <sub>CCINT</sub>						V <sub>CCBRAM</sub>				V <sub>CCAUX</sub>			V <sub>CCO</sub> Bank 0	V <sub>CCO</sub> all other Banks (per Bank)		
		680 $\mu$ F	330 $\mu$ F	100 $\mu$ F	47 $\mu$ F	4.7 $\mu$ F	0.47 $\mu$ F	100 $\mu$ F	47 $\mu$ F	4.7 $\mu$ F	0.47 $\mu$ F	47 $\mu$ F	4.7 $\mu$ F	0.47 $\mu$ F	47 $\mu$ F	47 $\mu$ F or 100 $\mu$ F <sup>(3)</sup>	4.7 $\mu$ F	0.47 $\mu$ F
CSG324	XC7A75T XA7A75T	0	1	0	0	4	6	1	0	0	2	1	2	4	1	1	2	4
CSG324	XC7A100T XQ7A100T XA7A100T	0	1	0	0	6	8	1	0	0	2	1	2	4	1	1	2	4
CSG325	XC7A15T XA7A15T	0	0	1	0	2	2	0	1	0	1	1	2	3	1	1	2	4
CSG325	XC7A35T XA7A35T	0	0	1	0	2	3	0	1	0	1	1	2	3	1	1	2	4
CSG325	XC7A50T XA7A50T XQ7A50T	0	1	0	0	3	5	1	0	0	1	1	2	3	1	1	2	4
FBG484 FBV484 RB484	XC7A200T XQ7A200T	1	0	0	0	12	14	1	0	0	3	1	3	5	1	1	2	4
FGG484	XC7A15T	0	0	1	0	2	2	0	1	0	1	1	2	5	1	1	2	4
FGG484	XC7A35T	0	0	1	0	2	3	0	1	0	1	1	2	5	1	1	2	4
FGG484	XC7A50T XQ7A50T	0	1	0	0	3	5	1	0	0	1	1	2	5	1	1	2	4
FGG484	XC7A75T XA7A75T	0	1	0	0	4	6	1	0	0	2	1	3	5	1	1	2	4
FGG484	XC7A100T XA7A100T XQ7A100T	0	1	0	0	6	8	1	0	0	2	1	3	5	1	1	2	4
SBG484 SBV484 RS484	XC7A200T XQ7A200T	1	0	0	0	12	14	1	0	0	3	1	3	5	1	1	2	4
FBG676 FBV676 RB676	XC7A200T XQ7A200T	1	0	0	0	12	14	1	0	0	3	1	4	7	1	1	2	4
FGG676	XC7A75T	0	1	0	0	4	6	1	0	0	2	1	3	5	1	1	2	4
FGG676	XC7A100T	0	1	0	0	6	8	1	0	0	2	1	3	5	1	1	2	4
FFG1156 FFV1156	XC7A200T	1	0	0	0	12	14	1	0	0	3	1	5	9	1	1	2	4

**Notes:**

1. PCB Capacitor specifications are listed in [Table 2-5](#).
2. Total includes all capacitors for all supplies, except for the MGT supplies MGTAVCC and MGTAVTT, which are covered in [UG482, 7 Series FPGAs GTP Transceivers User Guide](#). The values in this table account for the number of I/O banks in the device.
3. One 47  $\mu$ F (or 100  $\mu$ F) capacitor is required for up to four V<sub>CCO</sub> banks when powered by the same voltage.
4. Decoupling capacitors cover down to approximately 100 KHz.
5. Blank cells indicate that the data is not currently available.

Table 2-3 lists the PCB decoupling capacitor guidelines per V<sub>CC</sub> supply rail for Kintex-7 devices.



Table 2-3: Required PCB Capacitor Quantities per Device: Kintex-7 Devices<sup>(1)(2)</sup>

Package	Device	V <sub>CCINT</sub>			V <sub>CCBRAM</sub>				V <sub>CCAUX</sub>		V <sub>CCAUX_IO</sub> per Group <sup>(3)</sup>			V <sub>CCO</sub> Bank 0	V <sub>CCO</sub> all other Banks (per Bank)
		680 $\mu$ F	330 $\mu$ F	4.7 $\mu$ F	660 $\mu$ F	330 $\mu$ F	100 $\mu$ F	4.7 $\mu$ F	47 $\mu$ F	4.7 $\mu$ F	100 $\mu$ F	47 $\mu$ F	4.7 $\mu$ F	47 $\mu$ F	47 $\mu$ F or 100 $\mu$ F <sup>(4)</sup>
FBG484 FBV484	XC7K70T	0	1	0	0	0	1	2	2	3	N/A	N/A	N/A	1	1
FBG484 FBV484	XC7K160T	0	2	0	0	0	1	3	2	3	N/A	N/A	N/A	1	1
FBG676 FBV676	XC7K70T	0	1	0	0	0	1	2	2	3	0	0	0	1	1
FBG676 FBV676	XC7K160T	0	2	0	0	0	1	3	3	4	0	0	0	1	1
FBG676 FBV676	XC7K325T	0	3	5	0	0	2	5	3	4	0	0	0	1	1
FBG676 FBV676	XC7K410T	0	5	10	0	1	0	9	3	4	0	0	0	1	1
FBG900 FBV900	XC7K325T	0	3	5	0	0	2	5	4	4	0	0	0	1	1
FBG900 FBV900	XC7K410T	0	5	10	0	1	0	9	4	4	0	0	0	1	1
FFG676 FFV676	XC7K160T	0	2	0	0	0	1	3	2	0	0	1	0	1	1
FFG676 FFV676 RF676	XC7K325T XQ7K325T	0	3	0	0	0	2	5	2	0	0	1	0	1	1
FFG676 FFV676 RF676	XC7K410T XQ7K410T	0	5	0	0	1	0	9	2	0	0	1	0	1	1
FFG900 FFV900 RF900	XC7K325T XQ7K325T	0	3	0	0	0	2	5	3	0	0	1	0	1	1
FFG900 FFV900 RF900	XC7K410T XQ7K410T	0	5	0	0	1	0	9	3	0	0	1	0	1	1
FFG901 FFV901	XC7K355T	0	5	0	0	1	0	8	2	0	N/A	N/A	N/A	1	1
FFG901 FFV901	XC7K420T	0	5	0	0	1	0	9	3	0	N/A	N/A	N/A	1	1
FFG901 FFV901	XC7K480T	0	6	0	0	1	1	11	3	0	N/A	N/A	N/A	1	1
FFG1156 FFV1156	XC7K420T	0	5	0	0	1	0	9	3	0	N/A	N/A	N/A	1	1
FFG1156 FFV1156	XC7K480T	0	6	0	0	1	1	11	3	0	N/A	N/A	N/A	1	1

**Notes:**

1. PCB Capacitor specifications are listed in [Table 2-5](#).
2. Total includes all capacitors for all supplies, except for the MGT supplies MGTAVCC, MGTVCCAUX, and MGTAVTT, which are covered in [UG476, 7 Series FPGAs GTX/GTH Transceivers User Guide](#). The values in this table account for the number of I/O banks in the device.
3. See [UG471, 7 Series FPGAs SelectIO Resources User Guide](#) for a description of the VCCAUX\_IO rail specification to see which I/O banks are grouped together in each VCCAUX\_IO group. See [UG475, 7 Series FPGAs Packaging and Pinout Product Specification](#) to see which I/O banks are grouped together in each VCCAUX\_IO group.
4. One 47  $\mu$ F (or 100  $\mu$ F) capacitor is required for up to four V<sub>CCO</sub> banks when powered by the same voltage.
5. When N/A is listed for the VCCAUX\_IO per group, these components do not have HP I/O banks or VCCAUX\_IO pins.
6. Decoupling capacitors cover down to approximately 100 KHz.

Table 2-4 lists the PCB decoupling capacitor guidelines per  $V_{CC}$  supply rail for Virtex-7 devices.

Table 2-4: Required PCB Capacitor Quantities per Device: Virtex-7 Devices<sup>(1)(2)</sup>

Package	Device	$V_{CCINT}$			$V_{CCBRAM}$				$V_{CCAUX}$		$V_{CCAUX\_IO}$ per Group <sup>(3)</sup>			$V_{CC0}$ Bank 0	$V_{CC0}$ all other Banks (per Bank)
		680 $\mu F$	330 $\mu F$	4.7 $\mu F$	660 $\mu F$	330 $\mu F$	100 $\mu F$	4.7 $\mu F$	47 $\mu F$	4.7 $\mu F$	100 $\mu F$	47 $\mu F$	4.7 $\mu F$	47 $\mu F$	47 $\mu F$ or 100 $\mu F$ <sup>(4)</sup>
FFG1157 RF1157	XC7V585T XQ7V585T	3	0	0	0	1	0	9	1	0	1	0	0	1	1
FFG1157 FFV1157 RF1157	XC7VX330T XQ7VX330T	2	0	0	0	1	0	9	1	0	1	0	0	1	1
FFG1157 FFV1157	XC7VX415T	3	0	0	0	1	0	10	1	0	1	0	0	1	1
FFG1157	XC7VX485T	4	0	0	1	0	0	12	1	0	1	0	0	1	1
FFG1157 RF1157	XC7VX690T XQ7VX690T	5	0	0	1	0	0	17	1	0	1	0	0	1	1
FFG1158 FFV1158	XC7VX415T	3	0	0	0	1	0	10	1	0	1	0	0	1	1
FFG1158	XC7VX485T	4	0	0	1	0	0	12	1	0	1	0	0	1	1
FFG1158	XC7VX550T	4	0	0	1	0	0	13	1	0	1	0	0	1	1
FFG1158 RF1158	XC7VX690T	5	0	0	1	0	0	17	1	0	1	0	0	1	1
FFG1761 RF1761	XC7V585T XQ7V585T	3	0	0	0	1	0	9	1	0	1	0	0	1	1
FFG1761 FFV1761 RF1761	XC7VX330T XQ7VX330T	2	0	0	0	1	0	9	1	0	1	0	0	1	1
FFG1761 RF1761	XC7VX485T XQ7VX485T	4	0	0	1	0	0	12	1	0	1	0	0	1	1
FFG1761 RF1761	XC7VX690T XQ7VX690T	5	0	0	1	0	0	17	1	0	1	0	0	1	1
FHG1761	XC7V2000T	8	0	28	1	0	0	15	1	0	1	0	0	1	1
FLG1925	XC7V2000T	8	0	28	1	0	0	15	1	0	1	0	0	1	1
FFG1926	XC7VX690T	5	0	0	1	0	0	17	1	0	1	0	0	1	1
FFG1926	XC7VX980T	6	0	0	1	1	0	17	1	0	1	0	0	1	1
FLG1926	XC7VX1140T	6	0	0	1	0	0	21	1	0	1	0	0	1	1
FFG1927 FFV1927	XC7VX415T	3	0	0	0	1	0	10	1	0	1	0	0	1	1
FFG1927	XC7VX485T	4	0	0	1	0	0	12	1	0	1	0	0	1	1
FFG1927	XC7VX550T	4	0	0	1	0	0	13	1	0	1	0	0	1	1
FFG1927	XC7VX690T	5	0	0	1	0	0	17	1	0	1	0	0	1	1
FFG1928	XC7VX980T	6	0	0	1	1	0	20	1	0	1	0	0	1	1
FLG1928	XC7VX1140T	6	0	0	1	0	0	21	1	0	1	0	0	1	1
FFG1930 RF1930	XC7VX485T XQ7VX485T	4	0	0	1	0	0	12	1	0	1	0	0	1	1
FFG1930 RF1930	XC7VX690T XQ7VX690T	5	0	0	1	0	0	17	1	0	1	0	0	1	1

Table 2-4: Required PCB Capacitor Quantities per Device: Virtex-7 Devices<sup>(1)(2)</sup> (Continued)

Package	Device	V <sub>CCINT</sub>			V <sub>CCBRAM</sub>				V <sub>CCAUX</sub>		V <sub>CCAUX_IO</sub> per Group <sup>(3)</sup>			V <sub>CCO</sub> Bank 0	V <sub>CCO</sub> all other Banks (per Bank)
		680 $\mu$ F	330 $\mu$ F	4.7 $\mu$ F	660 $\mu$ F	330 $\mu$ F	100 $\mu$ F	4.7 $\mu$ F	47 $\mu$ F	4.7 $\mu$ F	100 $\mu$ F	47 $\mu$ F	4.7 $\mu$ F	47 $\mu$ F	47 $\mu$ F or 100 $\mu$ F <sup>(4)</sup>
FFG1930 RF1930	XC7VX980T XQ7VX980T	6	0	0	1	1	0	20	1	0	1	0	0	1	1
FLG1930	XC7VX1140T	6	0	0	1	0	0	21	1	0	1	0	0	1	1
FLG1155	XC7VH580T	3	0	0	1	0	0	11	1	0	1	0	0	1	1
FLG1931	XC7VH580T	3	0	0	1	0	0	11	1	0	1	0	0	1	1
FLG1932	XC7VH870T	5	0	0	1	1	0	16	1	0	1	0	0	1	1

**Notes:**

1. PCB Capacitor specifications are listed in Table 2-5.
2. Total includes all capacitors for all supplies, except for the MGT supplies MGTAVCC, MGTVCCAUX, and MGTAVTT, which are covered in UG476, 7 Series FPGAs GTX/GTH Transceivers User Guide. The values in this table account for the number of I/O banks in the device.
3. See UG471, 7 Series FPGAs SelectIO Resources User Guide for a description of the VCCAUX\_IO rail specification to see which I/O banks are grouped together in each VCCAUX\_IO group. See UG475, 7 Series FPGAs Packaging and Pinout Product Specification to see which I/O banks are grouped together in each VCCAUX\_IO group.
4. One 47  $\mu$ F (or 100  $\mu$ F) capacitor is required for up to four V<sub>CCO</sub> banks when powered by the same voltage.
5. Decoupling capacitors cover down to approximately 100 KHz.

## Capacitor Specifications

The electrical characteristics of the capacitors in Table 2-1, Table 2-2, Table 2-3, and Table 2-4 are specified in Table 2-5, and are followed by guidelines on acceptable substitutions. The equivalent series resistance (ESR) ranges specified for these capacitors can be over-ridden. However, this requires analysis of the resulting power distribution system impedance to ensure that no resonant impedance spikes result.

Table 2-5: PCB Capacitor Specifications

Ideal Value	Value Range <sup>(1)</sup>	Body Size <sup>(2)</sup>	Type	ESL Maximum	ESR Range <sup>(3)</sup>	Voltage Rating <sup>(4)</sup>	Suggested Part Number
680 $\mu$ F	C > 680 $\mu$ F	2917/D/ 7343	2-Terminal Tantalum	2.0 nH	5 m $\Omega$ < ESR < 40 m $\Omega$	2.5V	T530X687M006ATE018
330 $\mu$ F	C > 330 $\mu$ F	2917/D/ 7343	2-Terminal Tantalum	1 nH	5 m $\Omega$ < ESR < 40 m $\Omega$	2.5V	T520V337M2R5ATE025
330 $\mu$ F	C > 330 $\mu$ F	2917/D/ 7343	2-Terminal Niobium Oxide	1 nH	5 m $\Omega$ < ESR < 100 m $\Omega$	2.5V	NOSD337M002#0035
100 $\mu$ F	C > 100 $\mu$ F	1210	2-Terminal Tantalum Ceramic X7R or X5R	1 nH	1 m $\Omega$ < ESR < 40 m $\Omega$	2.5V	GRM32ER60J107ME20L
47 $\mu$ F	C > 47 $\mu$ F	1210	2-Terminal Ceramic X7R or X5R	1 nH	1 m $\Omega$ < ESR < 40 m $\Omega$	6.3V	GRM32ER70J476ME20L
4.7 $\mu$ F	C > 4.7 $\mu$ F	0805	2-Terminal Ceramic X7R or X5R	0.5 nH	1 m $\Omega$ < ESR < 20 m $\Omega$	6.3V	GRM21BR71A475KA73

Table 2-5: PCB Capacitor Specifications (Continued)

Ideal Value	Value Range <sup>(1)</sup>	Body Size <sup>(2)</sup>	Type	ESL Maximum	ESR Range <sup>(3)</sup>	Voltage Rating <sup>(4)</sup>	Suggested Part Number
0.47 $\mu$ F	$C > 0.47 \mu\text{F}$	0603	2-Terminal Ceramic X7R or X5R	0.5 nH	$1 \text{ m}\Omega < \text{ESR} < 20 \text{ m}\Omega$	6.3V	GRM188R70J474KA01

**Notes:**

1. Values can be larger than specified.
2. Body size can be smaller than specified.
3. ESR must be within the specified range.
4. Voltage rating can be higher than specified.

Table 2-6 lists the capacitors present in the packages for Kintex-7 devices.

Table 2-6: Package Capacitor Quantities per Device: Kintex-7 Devices<sup>(1)</sup>

Package	Device	$V_{CCINT}$	$V_{CCAUX}$	$V_{CCAUX\_IO}$ per Group <sup>(2)</sup>	$V_{CCO}$ per Bank <sup>(3)</sup>
		2.2 $\mu$ F	2.2 $\mu$ F	1.0 $\mu$ F	0.47 $\mu$ F
FBG484 FBV484	XC7K70T	2	1	N/A	1
FBG484 FBV484	XC7K160T	2	1	N/A	1
FBG676 FBV676	XC7K70T	2	1	N/A	1
FBG676 FBV676	XC7K160T	2	1	N/A	1
FBG676 FBV676	XC7K325T	2	1	1	1
FBG676 FBV676	XC7K410T	2	1	1	1
FBG900 FBV900	XC7K325T	2	1	1	1
FBG900 FBV900	XC7K410T	2	1	1	1
FFG676 FFV676	XC7K160T	4	2	1	1
FFG676 FFV676 RF676	XC7K325T XQ7K325T	4	2	1	1
FFG676 FFV676 RF676	XC7K410T XQ7K410T	4	2	1	1

Table 2-6: Package Capacitor Quantities per Device: Kintex-7 Devices<sup>(1)</sup> (Continued)

Package	Device	V <sub>CCINT</sub>	V <sub>CCAUX</sub>	V <sub>CCAUX_IO</sub> per Group <sup>(2)</sup>	V <sub>CCO</sub> per Bank <sup>(3)</sup>
		2.2 $\mu$ F	2.2 $\mu$ F	1.0 $\mu$ F	0.47 $\mu$ F
FFG900 FFV900 RF900	XC7K325T XQ7K325T	4	2	1	1
FFG900 FFV900 RF900	XC7K410T XQ7K410T	4	2	1	1
FFG901 FFV901	XC7K355T	4	2	N/A	1
FFG901 FFV901	XC7K420T	4	2	N/A	1
FFG901 FFV901	XC7K480T	4	2	N/A	1
FFG1156 FFV1156	XC7K420T	4	2	N/A	1
FFG1156 FFV1156	XC7K480T	4	2	N/A	1

**Notes:**

1. Total includes all capacitors for all supplies, except for the MGT supplies MGTAVCC, MGTVCCAUX, and MGTAVTT, which are covered in [UG476](#), 7 Series FPGAs GTX/GTH Transceivers User Guide. The values in this table account for the number of I/O banks in the device.
2. See [UG471](#), 7 Series FPGAs SelectIO Resources User Guide for a description of the VCCAUX\_IO rail specification. See [UG475](#), 7 Series FPGAs Packaging and Pinout Product Specification to see which I/O banks are grouped together in each VCCAUX\_IO group.
3. There are no package capacitors for V<sub>CCO</sub> bank 0.
4. When N/A is listed for the VCCAUX\_IO per group, these components do not have HP I/O banks or VCCAUX\_IO pins.

Table 2-7 shows the capacitor specifications for the Kintex-7 devices listed in Table 2-6.

Table 2-7: Capacitor Specifications for Kintex-7 Devices

Value ( $\mu$ F)	ESL (pH)	ESR (m $\Omega$ )
0.47	90	10
1.00	120	1000
2.20	60	16

Table 2-8 lists the capacitors present in the packages for Virtex-7 devices.

Table 2-8: Package Capacitor Quantities per Device: Virtex-7 Devices<sup>(1)</sup>

Package	Device	V <sub>CCINT</sub>	V <sub>CCAUX</sub>	VCCAUX_IO per group <sup>(2)</sup>	VCCO per Bank <sup>(3)</sup>
		4.7 $\mu$ F	4.7 $\mu$ F	1.0 $\mu$ F	0.47 $\mu$ F
FFG1157 RF1157	XC7V585T XQ7V585T	4	2	1	1
FFG1157 FFV1157 RF1157	XC7VX330T XQ7VX330T	4	2	1	1
FFG1157 FFV1157	XC7VX415T	4	2	1	1
FFG1157	XC7VX485T	4	2	1	1
FFG1157 RF1157	XC7VX690T XQ7VX690T	4	2	1	1
FFG1158 FFV1158	XC7VX415T	4	2	1	1
FFG1158	XC7VX485T	4	2	1	1
FFG1158	XC7VX550T	4	2	1	1
FFG1158 RF1158	XC7VX690T XQ7VX690T	4	2	1	1
FFG1761 RF1761	XC7V585T XQ7V585T	4	2	1	1
FFG1761 FFV1761 RF1761	XC7VX330T XQ7VX330T	4	2	1	1
FFG1761 RF1761	XC7VX485T XQ7VX485T	4	2	1	1
FFG1761 RF1761	XC7VX690T XQ7VX690T	4	2	1	1
FHG1761	XC7V2000T	6	2	1	1
FLG1925	XC7V2000T	6	2	1	1
FFG1926	XC7VX690T	4	2	1	1
FFG1926	XC7VX980T	4	2	1	1
FLG1926	XC7VX1140T	6	2	1	1
FFG1927 FFV1927	XC7VX415T	4	2	1	1
FFG1927	XC7VX485T	4	2	1	1
FFG1927	XC7VX550T	4	2	1	1

Table 2-8: Package Capacitor Quantities per Device: Virtex-7 Devices<sup>(1)</sup> (Continued)

Package	Device	V <sub>CCINT</sub>	V <sub>CCAUX</sub>	VCCAUX_IO per group <sup>(2)</sup>	V <sub>CCO</sub> per Bank <sup>(3)</sup>
		4.7 $\mu$ F	4.7 $\mu$ F	1.0 $\mu$ F	0.47 $\mu$ F
FFG1927	XC7VX690T	4	2	1	1
FFG1928	XC7VX980T	4	2	1	1
FLG1928	XC7VX1140T	6	2	1	1
FFG1930 RF1930	XC7VX485T XQ7VX485T	4	2	1	1
FFG1930 RF1930	XC7VX690T XQ7VX690T	4	2	1	1
FFG1930 RF1930	XC7VX980T XQ7VX980T	4	2	1	1
FLG1930	XC7VX1140T	6	2	1	1
FLG1155	XC7VH580T	4	2	1	1
FLG1931	XC7VH580T	6	2	1	1
FLG1932	XC7VH870T	6	2	1	1

**Notes:**

1. Total includes all capacitors for all supplies, except for the MGT supplies MGTAVCC, MGTVCCAUX, and MGTAVTT, which are covered in [UG476](#), 7 Series FPGAs GTX/GTH Transceivers User Guide. The values in this table account for the number of I/O banks in the device.
2. See [UG471](#), 7 Series FPGAs SelectIO Resources User Guide for a description of the VCCAUX\_IO rail specification. See [UG475](#), 7 Series FPGAs Packaging and Pinout Product Specification to see which I/O banks are grouped together in each VCCAUX\_IO group.
3. There are no package capacitors for V<sub>CCO</sub> bank 0.

Table 2-9 shows the capacitor specifications for the Virtex-7 devices listed in [Table 2-8](#).

Table 2-9: Capacitor Specifications for Virtex-7 Devices

Value ( $\mu$ F)	ESL (pH)	ESR (m $\Omega$ )
0.47	110	10
1.00	137	1000
4.7	70	5

## PCB Bulk Capacitors

The purpose of the bulk capacitors (D, 1210) is to cover the low-frequency range between where the voltage regulator stops working and where the on-package ceramic capacitors start working. As specified in [Table 2-1](#), [Table 2-2](#), [Table 2-3](#), and [Table 2-4](#), all FPGA supplies require bulk capacitors.

The tantalum and niobium oxide capacitors specified in [Table 2-5](#) were selected for their values and controlled ESR values. They are also ROHS compliant. If another manufacturer's tantalum, niobium oxide, or ceramic capacitors are used, the user must ensure they meet the specifications of [Table 2-5](#) and are properly evaluated via simulation, s-parameter parasitic extraction, or bench testing.

**Note:** If replacing a tantalum capacitor with a ceramic capacitor, the effective capacitance value can be reduced by approximately 50% under AC loading.

## PCB High-Frequency Capacitors

Table 2-5 shows the requirements for the 4.7  $\mu\text{F}$  capacitors in an 0805 package. Substitutions can be made for some characteristics, but not others. For details, refer to the notes in Table 2-5.

## Bulk Capacitor Consolidation Rules

Sometimes a number of I/O banks are powered from the same voltage (e.g., 1.8V) and the recommended guidelines call for multiple bulk capacitors. This is also the case for  $V_{\text{CCINT}}$ ,  $V_{\text{CCAUX}}$ ,  $V_{\text{CCAUX\_IO}}$ , and  $V_{\text{CCBRAM}}$  in the larger 7 series FPGAs. These many smaller capacitors can be consolidated into fewer (larger value) capacitors provided the electrical characteristics of the consolidated capacitors (ESR and ESL) are equal to the electrical characteristics of the parallel combination of the recommended capacitors.

For most consolidations of  $V_{\text{CCO}}$ ,  $V_{\text{CCINT}}$ ,  $V_{\text{CCAUX}}$ ,  $V_{\text{CCAUX\_IO}}$ , and  $V_{\text{CCBRAM}}$  capacitors, large tantalum capacitors with sufficiently low ESL and ESR are readily available.

## PCB Capacitor Placement and Mounting Techniques

### PCB Bulk Capacitors

Bulk capacitors (D, 1210) can be large and sometimes are difficult to place very close to the FPGA. Fortunately, this is not a problem because the low-frequency energy covered by bulk capacitors is not sensitive to capacitor location. Bulk capacitors can be placed almost anywhere on the PCB, but the best placement is as close as possible to the FPGA. Capacitor mounting should follow normal PCB layout practices, tending toward short and wide shapes connecting to power planes with multiple vias.

### 0805 and 0603 Ceramic Capacitors

The 0805 and 0603 capacitors cover the middle frequency range. Placement has some impact on their performance. The capacitors should be placed as close as possible to the FPGA. Any placement within two electrical inches of the device's point of load is acceptable. The capacitor mounting (solder lands, traces, and vias) should be optimized for low inductance. Vias should be butted directly against the pads. Vias can be located at the ends of the pads (see Figure 2-1B), but are more optimally located at the sides of the pads (see Figure 2-1C). Via placement at the sides of the pads decreases the mounting's overall parasitic inductance by increasing the mutual inductive coupling of one via to the other. Dual vias can be placed on both sides of the pads (see Figure 2-1D) for even lower parasitic inductance, but with diminishing returns.



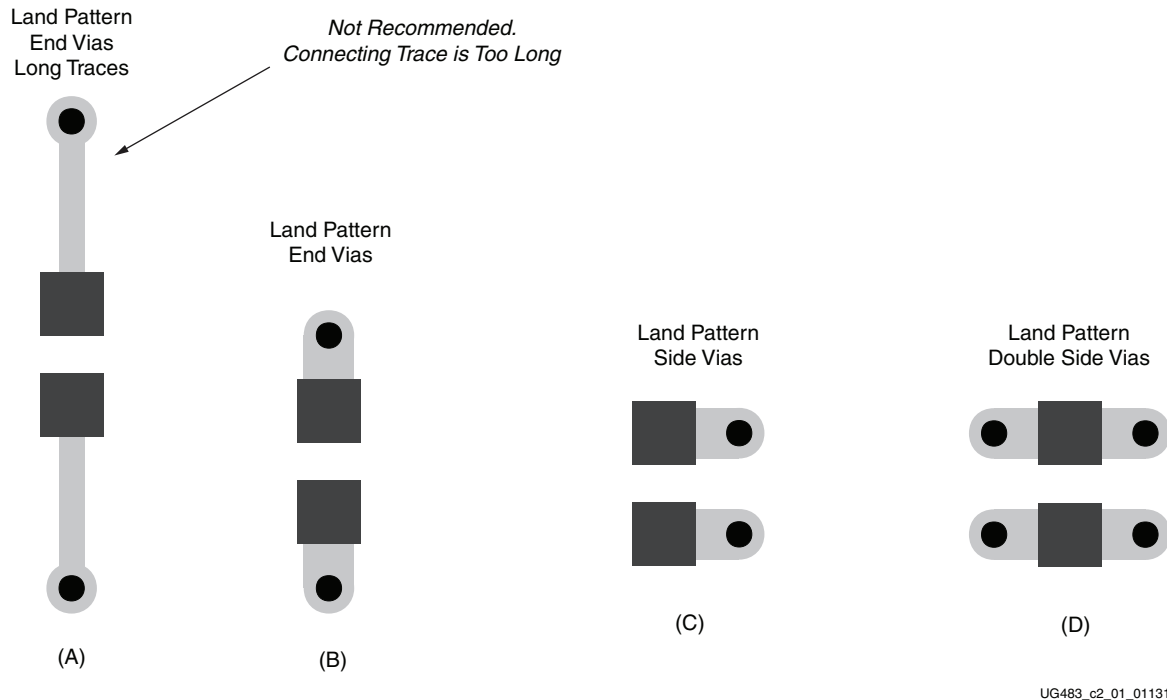


Figure 2-1: Example Capacitor Land and Mounting Geometries

## Basic PDS Principles

The purpose of the PDS and the properties of its components are discussed in this section. The important aspects of capacitor placement, capacitor mounting, PCB geometry, and PCB stackup recommendations are also described.

### Noise Limits

In the same way that devices in a system have a requirement for the amount of current consumed by the power system, there is also a requirement for the cleanliness of the power. This cleanliness requirement specifies a maximum amount of noise present on the power supply. Most digital devices, including all 7 series FPGAs, require that  $V_{CC}$  supplies not fluctuate more than the specifications documented in the device data sheet.

The power consumed by a digital device varies over time and this variance occurs on all frequency scales, creating a need for a wide-band PDS to maintain voltage stability.

- Low-frequency variance of power consumption is usually the result of devices or large portions of devices being enabled or disabled. This variance occurs in time frames from milliseconds to days.
- High-frequency variance of power consumption is the result of individual switching events inside a device. This occurs on the scale of the clock frequency and the first few harmonics of the clock frequency up to about 5 GHz.

Because the voltage level of  $V_{CC}$  for a device is fixed, changing power demands are manifested as changing current demand. The PDS must accommodate these variances of current draw with as little change as possible in the power-supply voltage.

When the current draw in a device changes, the PDS cannot respond to that change instantaneously. As a consequence, the voltage at the device changes for a brief period before the PDS responds. Two main causes for this PDS lag correspond to the two major PDS components: the voltage regulator and decoupling capacitors.

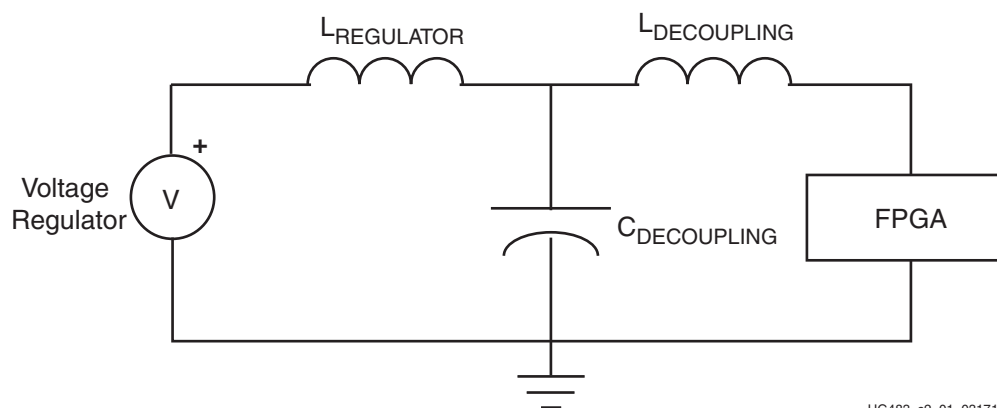
The first major component of the PDS is the voltage regulator. The voltage regulator observes its output voltage and adjusts the amount of current it is supplying to keep the output voltage constant. Most common voltage regulators make this adjustment in milliseconds to microseconds. Voltage regulators effectively maintain the output voltage for events at all frequencies from DC to a few hundred kHz, depending on the regulator (some are effective at regulating in the low MHz). For transient events that occur at frequencies above this range, there is a time lag before the voltage regulator responds to the new current demand level.

For example, if the device's current demand increases in a few hundred picoseconds, the voltage at the device sags by some amount until the voltage regulator can adjust to the new, higher level of required current. This lag can last from microseconds to milliseconds. A second component is needed to substitute for the regulator during this time, preventing the voltage from sagging.

This second major PDS component is the *decoupling* capacitor (also known as a bypass capacitor). The decoupling capacitor works as the device's local energy storage. The capacitor cannot provide DC power because it stores only a small amount of energy (voltage regulator provides DC power). This local energy storage should respond very quickly to changing current demands. The capacitors effectively maintain power-supply voltage at frequencies from hundreds of kHz to hundreds of MHz (in the milliseconds to nanoseconds range). Discrete decoupling capacitors are not useful for events occurring above or below this range.

For example, if current demand in the device increases in a few picoseconds, the voltage at the device sags by some amount until the capacitors can supply extra charge to the device. If current demand in the device maintains this new level for many milliseconds, the voltage-regulator circuit, operating in parallel with the decoupling capacitors, replaces the capacitors by changing its output to supply this new level of current.

Figure 2-2 shows the major PDS components: the voltage regulator, the decoupling capacitors, and the active device being powered (FPGA).



UG483\_c2\_01\_031711

Figure 2-2: Simplified PDS Circuit

Figure 2-3 shows a simplified PDS circuit with all reactive components represented by a frequency-dependent resistor.

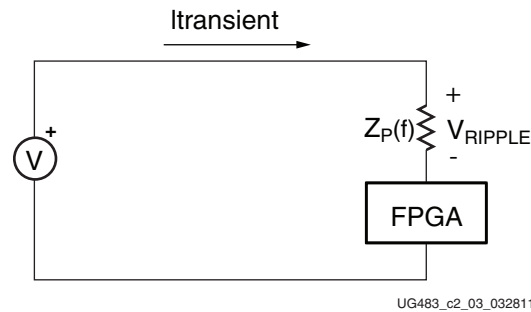


Figure 2-3: Further Simplified PDS Circuit

## Role of Inductance

Inductance is the property of the capacitors and the PCB current paths that slows down changes in current flow. Inductance is the reason why capacitors cannot respond instantaneously to transient currents or to changes that occur at frequencies higher than their effective range.

Inductance can be thought of as the momentum of charge. Charge moving through a conductor represents some amount of current. If the level of current changes, the charge moves at a different rate. Because momentum (stored magnetic-field energy) is associated with this charge, some amount of time and energy is required to slow down or speed up the charge flow. The greater the inductance, the greater the resistance to change, and the longer the time required for the current level to change. A voltage develops across the inductance as this change occurs.

The PDS, made up of a regulator and multiple stages of decoupling capacitors, accommodates the device current demand and responds to current transients as quickly as necessary to maintain the voltage within the specified limits. When these current demands are not met, the voltage across the device's power supply changes. This is observed as noise. Inductance in the current path of the capacitors should be minimized, because it retards the ability of decoupling capacitors to quickly respond to changing current demands.

Inductances occur between the FPGA device and capacitors and between the capacitors and the voltage regulator (see Figure 2-2). These inductances occur as parasitics in the capacitors and in all PCB current paths. It is important that each of these parasitics be minimized.

## Capacitor Parasitic Inductance

The capacitance value is often considered to be a capacitors's most important characteristic. In power system applications, the parasitic inductance (ESL) has the same or greater importance. Capacitor package dimensions (body size) determine the amount of parasitic inductance. Physically small capacitors usually have lower parasitic inductance than physically large capacitors.

Requirements for choosing decoupling capacitors:

- For a specific capacitance value, choose the smallest package available.
- or -
- For a specific package size (essentially a fixed inductance value), choose the highest capacitance value available in that package.

Surface-mount chip capacitors are the smallest capacitors available and are a good choice for discrete decoupling capacitors:

- For values from 100  $\mu\text{F}$  to very small values such as 0.01  $\mu\text{F}$ , ceramic X7R or X5R type capacitors are usually used. These capacitors have a low parasitic inductance and a low ESR, with an acceptable temperature characteristic.
- For larger values, such as 47  $\mu\text{F}$  to 1000  $\mu\text{F}$ , tantalum capacitors are usually used. These capacitors have a low parasitic inductance and a medium ESR, giving them a low Q factor and consequently a very wide range of effective frequencies.

If tantalum capacitors are not available or cannot be used, low-ESR, low-inductance electrolytic capacitors can be used, provided they have comparable ESR and ESL values. Other new technologies with similar characteristics are also available (Os-Con, POSCAP, and Polymer-Electrolytic SMT).

A *real* capacitor of any type then not only has capacitance characteristics but also inductance and resistance characteristics. Figure 2-4 shows the parasitic model of a real capacitor. A real capacitor should be treated as an *RLC circuit* (a circuit consisting of a resistor (R), an inductor (L), and a capacitor (C), connected in series).

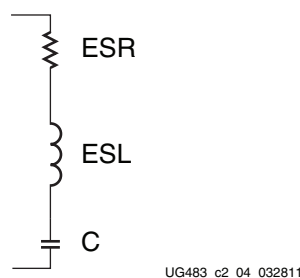


Figure 2-4: Parasitics of a Real, Non-Ideal Capacitor

Figure 2-5 shows a *real* capacitor's impedance characteristic. Overlaid on this plot are curves corresponding to the capacitor's capacitance and parasitic inductance (ESL). These two curves combine to form the RLC circuit's total impedance characteristic, softened or sharpened by the capacitor's ESR.

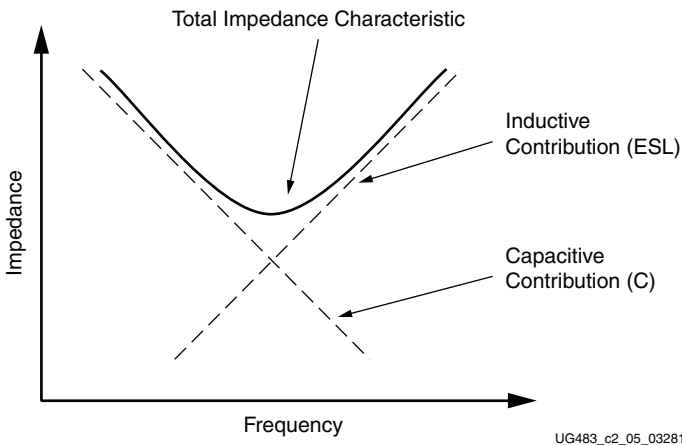


Figure 2-5: Contribution of Parasitics to Total Impedance Characteristics

As capacitive value is increased, the capacitive curve moves down and left. As parasitic inductance is decreased, the inductive curve moves down and right. Because parasitic

inductance for capacitors in a specific package is fixed, the inductance curve for capacitors in a specific package remains fixed.

As different capacitor values are selected in the same package, the capacitive curve moves up and down against the fixed inductance curve, as shown in Figure 2-6.

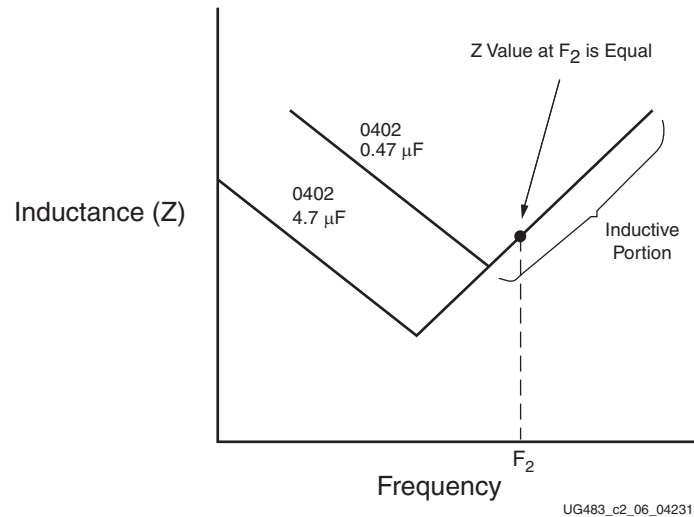


Figure 2-6: Effective Frequency Example

The low-frequency capacitor impedance can be reduced by increasing the value of the capacitor; the high-frequency impedance can be reduced by decreasing the inductance of the capacitor. While it might be possible to specify a higher capacitance value in the fixed package, it is not possible to lower the inductance of the capacitor (in the fixed package) without putting more capacitors in parallel. Using multiple capacitors in parallel divides the parasitic inductance, and at the same time, multiplies the capacitance value. This lowers both the high and low frequency impedance at the same time.

## PCB Current Path Inductance

The parasitic inductance of current paths in the PCB have three distinct sources:

- Capacitor mounting
- PCB power and ground planes
- FPGA mounting

### Capacitor Mounting Inductance

Capacitor mounting refers to the capacitor's solder lands on the PCB, the trace (if any) between the land and via, and the via.

The vias, traces, and capacitor mounting pads of a 2-terminal capacitor contribute inductance between 300 pH to 4 nH depending on the specific geometry.

Because the current path's inductance is proportional to the loop area the current traverses, it is important to minimize this loop size. The loop consists of the path through one power plane, up through one via, through the connecting trace to the land, through the capacitor, through the other land and connecting trace, down through the other via, and into the other plane, as shown in Figure 2-7.

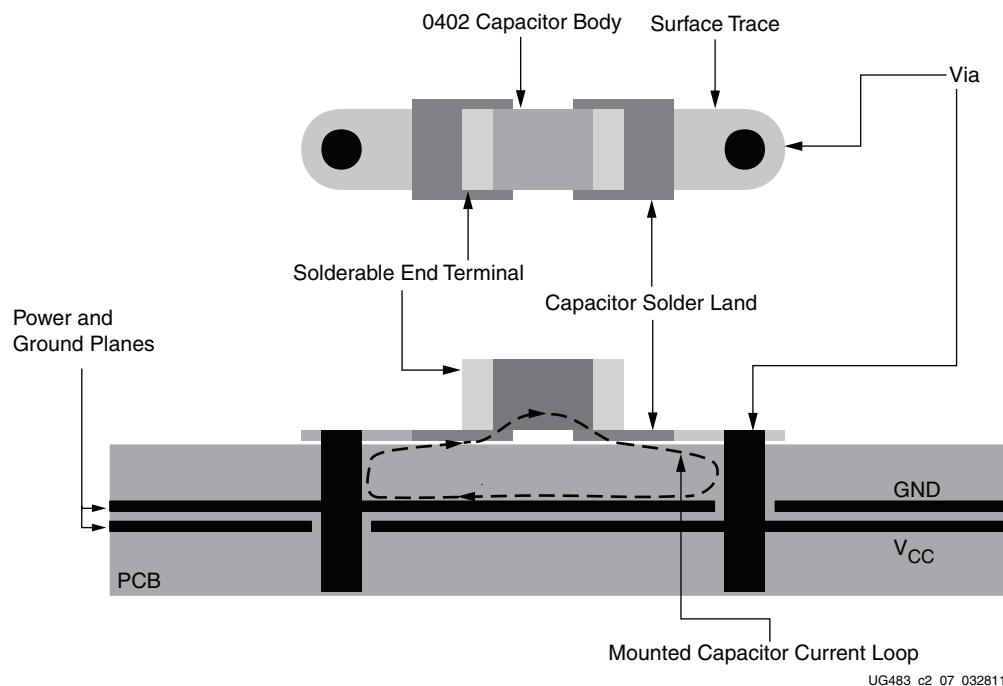


Figure 2-7: Example Cutaway View of PCB with Capacitor Mounting

A connecting trace length has a large impact on the mounting's parasitic inductance and if used, should be as short and wide as possible. When possible, a connecting trace should *not* be used and the via should butt up against the land. Placing vias to the side of the capacitor lands or doubling the number of vias, further reduces the mounting's parasitic inductance.

Some PCB manufacturing processes allow via-in-pad geometries, an option for reducing parasitic inductance. Using multiple vias per land is important with ultra-low inductance capacitors, such as reverse aspect ratio capacitors that place wide terminals on the sides of the capacitor body instead of the ends.

PCB layout engineers often try to squeeze more parts into a small area by sharing vias among multiple capacitors. *This technique should not be used under any circumstances.* PDS improvement is very small when a second capacitor is connected to an existing capacitor's vias. For a larger improvement, reduce the total number of capacitors and maintain a one-to-one ratio of lands to vias.

The capacitor mounting (lands, traces, and vias) typically contributes about the same amount or more inductance than the capacitor's own parasitic self-inductance.

## Plane Inductance

Some inductance is associated with the PCB power and ground planes. The geometry of these planes determines their inductance.

Current spreads out as it flows from one point to another (due to a property similar to *skin effect*) in the power and ground planes. Inductance in planes can be described as *spreading inductance* and is specified in units of henries per square. The square is dimensionless; the shape of a section of a plane, not the size, determines the amount of inductance.

Spreading inductance acts like any other inductance and resists changes to the amount of current in a power plane (the conductor). The inductance retards the capacitor's ability to respond to a device's transient currents and should be reduced as much as possible. Because the designer's control over the X-Y shape of the plane can be limited, the only controllable factor is the spreading inductance value. This is determined by the thickness of the dielectric separating a power plane from its associated ground plane.

For high-frequency power distribution systems, power and ground planes work in pairs, with their inductances coexisting dependently with each other. The spacing between the power and ground planes determines the pair's spreading inductance. The closer the spacing (the thinner the dielectric), the lower the spreading inductance. Approximate values of spreading inductance for different thicknesses of FR4 dielectric are shown in [Table 2-10](#).

**Table 2-10: Capacitance and Spreading Inductance Values for Different Thicknesses of FR4 Power-Ground Plane Sandwiches**

Dielectric Thickness		Inductance	Capacitance	
(micron)	(mil)	(pH/square)	(pF/in <sup>2</sup> )	(pF/cm <sup>2</sup> )
102	4	130	225	35
51	2	65	450	70
25	1	32	900	140

Decreased spreading inductance corresponds to closer spacing of  $V_{CC}$  and GND planes. When possible, place the  $V_{CC}$  planes directly adjacent to the GND planes in the PCB stackup. Facing  $V_{CC}$  and GND planes are sometimes referred to as *sandwiches*. While the use of  $V_{CC}$  – GND sandwiches was not necessary in the past for previous technologies (lead frames, wire bond packages), the speeds involved and the sheer amount of power required for fast, dense devices often demand it.

However, because of the presence of substrate decoupling capacitors in 7 series FPGAs, there is a limit to the amount of fast transient current demanded from PCB decoupling capacitors. This means that there is little benefit from dielectric thicknesses below 50 $\mu$  (2 mil). Dielectric thickness of 50 $\mu$  or 75 $\mu$  between  $V_{CC}$  and GND layers is sufficient for 7 series FPGAs.

Besides offering a low-inductance current path, power-ground sandwiches also offer some high-frequency decoupling capacitance. As the plane area increases and as the separation between power and ground planes decreases, the value of this capacitance increases. Capacitance per square inch is shown in [Table 2-10](#). However, the amount of capacitance arising from these PCB power-ground plane pairs is generally inconsequential, given the substrate decoupling capacitors present in 7 series FPGAs.

## FPGA Mounting Inductance

The PCB solder lands and vias that connect the FPGA power pins ( $V_{CC}$  and GND) contribute an amount of parasitic inductance to the overall power circuit. For existing PCB technology, the solder land geometry and the dogbone geometry are mostly fixed, and parasitic inductance of these geometries does not vary. Via parasitic inductance is a function of the via length and the proximity of the opposing current paths to one another.

The relevant via length is the portion of the via that carries transient current between the FPGA solder land and the associated  $V_{CC}$  or GND plane. Any remaining via (between the power plane and the PCB backside) does not affect the parasitic inductance of the via (the shorter the via between the solder lands and the power plane, the smaller the parasitic

inductance). Parasitic via inductance in the FPGA mounting is reduced by keeping the relevant  $V_{CC}$  and GND planes as close to the FPGA as possible (close to the top of the PCB stackup).

Device pinout arrangement determines the proximity of opposing current paths to one another. Inductance is associated with any two opposing currents (for example, current flowing in a  $V_{CC}$  and GND via pair). A high degree of mutual inductive coupling between the two opposing paths reduces the loop's total inductance. Therefore, when given a choice,  $V_{CC}$  and GND vias should be as close together as possible.

The via field under an FPGA has many  $V_{CC}$  and GND vias, and the total inductance is a function of the proximity of one via to another:

- For core  $V_{CC}$  supplies ( $V_{CCINT}$  and  $V_{CCAUX}$ ), opposing current is between the  $V_{CC}$  and GND pins.
- For I/O  $V_{CC}$  supplies ( $V_{CCO}$ ), opposing current is between any I/O and its return current path, whether carried by a  $V_{CCO}$  or GND pin.

To reduce parasitic inductance:

- Core  $V_{CC}$  pins such as  $V_{CCINT}$  and  $V_{CCAUX}$  are placed in a checkerboard arrangement in the pinout.
- $V_{CCO}$  and GND pins are distributed among the I/O pins.

Every I/O pin in the 7 series FPGA pinout is adjacent to a return-current pin.

FPGA pinout arrangement determines the PCB via arrangement. The PCB designer cannot control the proximity of opposing current paths but has control over the trade-offs between the capacitor's mounting inductance and FPGA's mounting inductance:

- Both mounting inductances are reduced by placing power planes close to the PCB stackup's top half and placing the capacitors on the top surface (reducing the capacitor's via length).
- If power planes are placed in the PCB stackup's bottom half, the capacitors must be mounted on the PCB backside. In this case, FPGA mounting vias are already long, and making the capacitor vias long (by coming down from the top surface) is a bad practice. A better practice is to take advantage of the short distance between the underside of the PCB and the power plane of interest, mounting capacitors on the underside.

## PCB Stackup and Layer Order

$V_{CC}$  and ground plane placement in the PCB stackup (the layer order) has a significant impact on the parasitic inductances of power current paths. Layer order must be considered early in the design process:

- High-priority supplies should be placed closer to the FPGA (in the PCB stackup's top half)
- Low-priority supplies should be placed farther from the FPGA (in the PCB stackup's bottom half)

Power supplies with high transient current should have the associated  $V_{CC}$  planes close to the top surface (FPGA side) of the PCB stackup. This decreases the vertical distance ( $V_{CC}$  and GND via length) that currents travel before reaching the associated  $V_{CC}$  and GND planes. To reduce spreading inductance, every  $V_{CC}$  plane should have an adjacent GND plane in the PCB stackup. The skin effect causes high-frequency currents to couple tightly, and the GND plane adjacent to a specific  $V_{CC}$  plane tends to carry the majority of the



current complementary to that in the  $V_{CC}$  plane. Thus, adjacent  $V_{CC}$  and GND planes are treated as a pair.

Not all  $V_{CC}$  and GND plane pairs reside in the PCB stackup's top half because manufacturing constraints typically require a symmetrical PCB stackup around the center (with respect to dielectric thicknesses and etched copper areas). The PCB designer chooses the priority of the  $V_{CC}$  and GND plane pairs: high priority pairs carry high transient currents and are placed high in the stackup, while low priority pairs carry lower transient currents (or can tolerate more noise) and are placed in the lower part of the stackup.

## Capacitor Effective Frequency

Every capacitor has a narrow frequency band where it is most effective as a decoupling capacitor. This band is centered at the capacitor's self-resonant frequency  $F_{RSELF}$ . The effective frequency bands of some capacitors are wider than others. A capacitor's ESR determines the capacitor's quality (Q) factor, and the Q factor can determine the width of the effective frequency band:

- Tantalum capacitors generally have a very *wide* effective band.
- Ceramic chip capacitors with a lower ESR, generally have a very *narrow* effective frequency band.

An ideal capacitor only has a capacitive characteristic, whereas *real* non-ideal capacitors also have a parasitic inductance (ESL) and a parasitic resistance (ESR). These parasitics work in series to form an RLC circuit (Figure 2-4). The RLC circuit's resonant frequency is the capacitor's self-resonant frequency.

To determine the RLC circuit's resonant frequency, use Equation 2-1:

$$F = \frac{1}{2\pi\sqrt{LC}} \quad \text{Equation 2-1}$$

Another method of determining the self-resonant frequency is to find the minimum point in the impedance curve of the equivalent RLC circuit. The impedance curve can be computed or generated in SPICE using a frequency sweep. See the [Simulation Methods](#) section for other ways to compute an impedance curve.

It is important to distinguish between the capacitor's self-resonant frequency and the mounted capacitor's effective resonant frequency when the capacitor is part of the system,  $F_{RIS}$ . This corresponds to the resonant frequency of the capacitor with its parasitic inductance, plus the inductance of the vias, planes, and connecting traces between the capacitor and the FPGA.

The capacitor's self-resonant frequency,  $F_{RSELF}$ , (capacitor data sheet value) is much higher than its effective mounted resonant frequency in the system,  $F_{RIS}$ . Because the mounted capacitor's performance is most important, the mounted resonant frequency is used when evaluating a capacitor as part of the greater PDS.

Mounted parasitic inductance is a combination of the capacitor's own parasitic inductance and the inductance of: PCB lands, connecting traces, vias, and power planes. Vias traverse a full PCB stackup to the device when capacitors are mounted on the PCB backside. For a board with a finished thickness of 1.524 mm (60 mils), these vias contribute approximately 300 pH to 1,500 pH, (the capacitor's mounting parasitic inductance,  $L_{MOUNT}$ ) depending on the spacing between vias. Wider-spaced vias and vias in thicker boards have higher inductance.

To determine the capacitor's total parasitic inductance in the system,  $L_{IS}$ , the capacitor's parasitic inductance,  $L_{SELF}$ , is added to the mounting's parasitic inductance,  $L_{MOUNT}$ :

$$L_{IS} = L_{SELF} + L_{MOUNT} \quad \text{Equation 2-2}$$

For example, using X7R Ceramic Chip capacitor in 0402 body size:

$C = 0.01 \mu\text{F}$  (selected by user)

$L_{SELF} = 0.9 \text{ nH}$  (capacitor data sheet parameter)

$F_{RSELF} = 53 \text{ MHz}$  (capacitor data sheet parameter)

$L_{MOUNT} = 0.8 \text{ nH}$  (based on PCB mounting geometry)

To determine the effective in-system parasitic inductance ( $L_{IS}$ ), add the via parasitics:

$$\begin{aligned} L_{IS} &= L_{SELF} + L_{MOUNT} = 0.9 \text{ nH} + 0.8 \text{ nH} \\ L_{IS} &= 1.7 \text{ nH} \end{aligned} \quad \text{Equation 2-3}$$

The values from the example are used to determine the mounted capacitor resonant frequency ( $F_{RIS}$ ). Using Equation 2-1:

$$F_{RIS} = \frac{1}{2\pi\sqrt{L_{IS}C}} \quad \text{Equation 2-4}$$

$$F_{RIS} = \frac{1}{2\pi\sqrt{(1.7 \times 10^{-9} \text{ H}) \cdot (0.01 \times 10^{-6} \text{ F})}} = 38 \times 10^6 \text{ Hz} \quad \text{Equation 2-5}$$

$F_{RSELF}$  is 53 MHz, but  $F_{RIS}$  is lower at 38 MHz. The addition of mounting inductances shifts the effective-frequency band down.

A decoupling capacitor is most effective at the narrow-frequency band around its resonant frequency, and thus, the resonant frequency must be reviewed when choosing a capacitor collection to build up a decoupling network. This being said, capacitors can be effective at frequencies considerably higher and lower than their resonant frequency. Recall that capacitors of differing values in the same package share the same inductance curve. As shown in Figure 2-6, for any given frequency along the inductive portion of the curve, the capacitors are equally effective.

## Capacitor Anti-Resonance

One problem associated with combinations of capacitors in a PDS of an FPGA is anti-resonant spikes in the PDS aggregate impedance. The cause for these spikes is a bad combination of energy storage elements in the PDS (intrinsic capacitances, discrete capacitors, parasitic inductances, and power and ground planes).

Anti-resonance can arise between any two consecutive stages of a power distribution system, such as between the high-frequency PCB capacitors and the PCB plane capacitance. The inter-plane capacitance of the power and ground planes generally has a high-Q factor. If the high-frequency PCB capacitors also are high-Q, the crossover point between the high-frequency discrete capacitors and the plane capacitance might exhibit a high-impedance anti-resonance peak. If the FPGA has a high transient current demand at this frequency (as a stimulus), a large noise voltage can occur.

To correct this type of problem, the characteristics of the high-frequency discrete capacitors or the characteristics of the  $V_{CC}$  and ground planes must be changed, or FPGA activity shifted to a different frequency away from the resonance.

## Capacitor Placement Background

To perform the decoupling function, capacitors should be close to the device being decoupled.

Increased spacing between the FPGA and decoupling capacitor increases the current flow distance in the power and ground planes, and it often increases the current path's inductance between the device and the capacitor.

The inductance of this current path (the loop followed by current as it travels from the  $V_{CC}$  side of the capacitor to the  $V_{CC}$  pin[s] of the FPGA, and from the GND pin[s] of the FPGA to the GND side of the capacitor[s]), is proportional to the loop area. Inductance is decreased by decreasing the loop area.

Shortening the distance between the device and the decoupling capacitor reduces the inductance, resulting in a less impeded transient current flow. Because of typical PCB dimensions, this lateral plane travel tends to be less important than the phase relationship between the FPGA noise source and the mounted capacitor.

The phase relationship between the FPGA's noise source and the mounted capacitor determines the capacitor's effectiveness. For a capacitor to be effective in providing transient current at a certain frequency (for example, the capacitor's resonant frequency), the phase relationship, based on the distance travelled by the current from the FPGA to the capacitor, must be within a fraction of the corresponding period.

The capacitor's placement determines the length of the transmission line interconnect (in this case, the power and ground plane pair) between the capacitor and FPGA. The propagation delay of this interconnect is the key factor.

FPGA noise falls into certain frequency bands, and different sizes of decoupling capacitors take care of different frequency bands. Thus, capacitor placement requirements are determined by each capacitor's effective frequency.

When the FPGA initiates a current demand change, it causes a small local disturbance in the PDS voltage (a point in the power and ground planes). Before it can counteract this, the decoupling capacitor must first sense a voltage difference.

A finite time delay ([Equation 2-6](#)) occurs between the start of the disturbance at the FPGA power pins and the point when the capacitor senses the disturbance.

$$\text{Time Delay} = \frac{\text{Distance from the FPGA power pins to the capacitor}}{\text{Signal propagation speed through FR4 dielectric}} \quad \text{Equation 2-6}$$

The dielectric is the substrate of the PCB where the power planes are embedded.

Another delay of the same duration occurs when the compensation current from the capacitor flows to the FPGA. For any transient current demand in the FPGA, a round-trip delay occurs before any relief is seen at the FPGA.

- Negligible energy is transferred to the FPGA with placement distances greater than one quarter of a demand frequency's wavelength.
- Energy transferred to the FPGA increases from 0% at one-quarter of a wavelength to 100% at zero distance.
- Energy is transferred efficiently from the capacitor to the FPGA when capacitor placement is at a fraction of a quarter wavelength of the FPGA power pins. This fraction should be small because the capacitor is also effective at some frequencies (shorter wavelengths) above its resonant frequency.

One-tenth of a quarter wavelength is a good target for most practical applications and leads to placing a capacitor within one-fortieth of a wavelength of the power pins it is decoupling. The wavelength corresponds to the capacitor's mounted resonant frequency,  $F_{\text{RIS}}$ .

When using large numbers of external termination resistors or passive power filtering for transceivers, priority should be given to these over the decoupling capacitors. Moving away from the device in concentric rings, the termination resistors and transceiver supply filtering should be closest to the device, followed by the smallest-value decoupling capacitors, then the larger-value decoupling capacitors.

## $V_{\text{REF}}$ Stabilization Capacitors

In  $V_{\text{REF}}$  supply stabilization, one capacitor per pin is placed as close as possible to the  $V_{\text{REF}}$  pin. The capacitors used are in the 0.022  $\mu\text{F}$  – 0.47  $\mu\text{F}$  range. The  $V_{\text{REF}}$  capacitor's primary function is to reduce the  $V_{\text{REF}}$  node impedance, which in turn reduces crosstalk coupling. Since no low-frequency energy is needed, larger capacitors are not necessary.

This only applies when Internal  $V_{\text{REF}}$  is not used. Internal  $V_{\text{REF}}$  is a feature in the 7 series FPGAs wherein the reference voltage rail is generated internally, which in turn allows the  $V_{\text{REF}}$  pins to be used as regular I/O pins. See [UG471](#), *7 Series FPGAs SelectIO User Guide* for more details on Internal  $V_{\text{REF}}$ .

## Power Supply Consolidation

Powering 1.8V  $V_{\text{CCO}}$ ,  $V_{\text{CCAUX}}$ , and  $V_{\text{CCAUX}_{\text{IO}}}$  from a common PCB plane is allowed in 7 series FPGA designs. However, careful consideration must be given to power supply noise—in particular, any noise on the  $V_{\text{CCO}}$  rail should not violate the recommended operating condition range for the  $V_{\text{CCAUX}}$  supply. See [DS182](#), *Kintex-7 FPGAs Data Sheet: DC and Switching Characteristics* and [DS183](#), *Virtex®-7 FPGAs Data Sheet: DC and Switching Characteristics* for these requirements.

## Unconnected $V_{\text{CCO}}$ Pins

In some cases, one or more I/O banks in an FPGA are not used (for example, when an FPGA has far more I/O pins than the design requires). In these cases, it might be desirable to leave the bank's associated  $V_{\text{CCO}}$  pins unconnected, as it can free up some PCB layout constraints (less voiding of power and ground planes from via antipads, less obstacles to signals entering and exiting the pinout array, more copper area available for other planelets in the otherwise used plane layer).

Leaving the  $V_{\text{CCO}}$  pins of unused I/O banks floating reduces the level of ESD protection on these pins and the I/O pins in the bank. For maximum ESD protection in an unused bank, all  $V_{\text{CCO}}$  and I/O pins in that bank should be connected together to the same potential, whether that be ground, a valid  $V_{\text{CCO}}$  voltage, or a floating plane.

## Simulation Methods

Simulation methods, ranging from very simple to very complex, exist to predict the PDS characteristics. An accurate simulation result is difficult to achieve without using a fairly sophisticated simulator and taking a significant amount of time.

Basic lumped RLC simulation is one of the simplest simulation methods. Though it does not account for the distributed behavior of a PDS, it is a useful tool for selecting and verifying that combinations of decoupling capacitor values will not lead to large anti-

resonances. Lumped RLC simulation is a good method for establishing equivalence of decoupling networks, such as evaluating an alternative to the capacitors of [Table 2-5](#).

Lumped RLC simulation is performed either in a version of SPICE or other circuit simulator, or by using a mathematical tool like MathCAD or Microsoft Excel. Istvan Novak publishes a free Excel spreadsheet for lumped RLC simulation (among other useful tools for PDS simulation) on his website under **Tool Download**:

<http://www.electrical-integrity.com>

[Table 2-11](#) also lists a few EDA tool vendors for PDS design and simulation. These tools span a wide range of sophistication levels.

**Table 2-11: EDA Tools for PDS Design and Simulation**

Tool	Vendor	Website URL
ADS	Cadence	<a href="http://www.cadence.com">http://www.cadence.com</a>
SIwave, HFSS	Ansoft	<a href="http://www.ansoft.com">http://www.ansoft.com</a>
Specctraquest Power Integrity	Cadence	<a href="http://www.cadence.com">http://www.cadence.com</a>
Speed 2000, PowerSI, PowerDC	Cadence	<a href="http://www.cadence.com">http://www.cadence.com</a>
Hyperlynx PI	Mentor	<a href="http://www.mentor.com">http://www.mentor.com</a>

## PDS Measurements

Measurements can be used to determine whether a PDS is adequate. PDS noise measurements are a unique task, and many specialized techniques have been developed. This section describes the noise magnitude and noise spectrum measurements.

### Noise Magnitude Measurement

Noise measurement must be performed with a high-bandwidth oscilloscope (minimum 3 GHz oscilloscope and 1.5 GHz probe or direct coaxial connection) on a design running realistic test patterns. The measurement is taken at the device's power pins or at an unused I/O driven High or Low (referred to as a *spyhole measurement*).

$V_{CCINT}$  and  $V_{CCAUX}$  can only be measured at the PCB backside vias.  $V_{CCO}$  can also be measured this way, but more accurate results are obtained by measuring static (fixed logic level) signals at unused I/Os in the bank of interest.

When making the noise measurement on the PCB backside, the via parasitics in the path between the measuring point and FPGA must be considered. Any voltage drop occurring in this path is not accounted for in the oscilloscope measurement.

PCB backside via measurements also have a potential problem: decoupling capacitors are often mounted directly underneath the device, meaning the capacitor lands connect directly to the  $V_{CC}$  and GND vias with surface traces. These capacitors confuse the measurement by acting like a short circuit for the high-frequency AC current. To make sure the measurements are not shorted by the capacitors, remove the capacitor at the measurement site (keep all others to reflect the real system behavior).

When measuring  $V_{CCO}$  noise, the measurement can be taken at an I/O pin configured as a driver to logic 1 or logic 0. In most cases, the same I/O standard should be used for this "spyhole" as for the other signals in the bank. Measuring a static logic 0 shows the crosstalk (via field, PCB routing, package routing) induced on the victim. Measuring a static logic 1 shows all the same crosstalk components as well as the noise present on the  $V_{CCO}$  net for the I/O bank. By subtracting (coherently in time) the noise measured on static logic 0 from the noise measured on static logic 1, the noise on  $V_{CCO}$  at the die can be viewed. For an accurate result, the static logic 0 and static logic 1 noise must be measured at the same I/O location. This means storing the time-domain waveform information from both logic states and performing the subtraction operation on the two waveforms in a post-process math computation tool such as MATLAB or Excel.

#### Oscilloscope Measurement Methods

There are two basic ways of using the oscilloscope to view power system noise, each for a different purpose. The first surveys all possible noise events, while the second is useful for focusing on individual noise sources.

- Place the oscilloscope in infinite persistence mode to acquire all noise over a long time period (many seconds or minutes). If the design operates in many different modes, using different resources in different amounts, these various conditions and modes should be in operation while the oscilloscope is acquiring the noise measurement.
- Place the oscilloscope in averaging mode and trigger on a known aggressor event. This can show the amount of noise correlated with the aggressor event (any events asynchronous to the aggressor are removed through averaging).

Power system noise measurements should be made at a few different FPGA locations to ensure that any local noise phenomena are captured.

Figure 2-8 shows an averaged noise measurement taken at the  $V_{CC0}$  pins of a sample design. In this case, the trigger was the clock for an I/O bus interface sending a 1-0-1-0 pattern at 250 Mb/s.

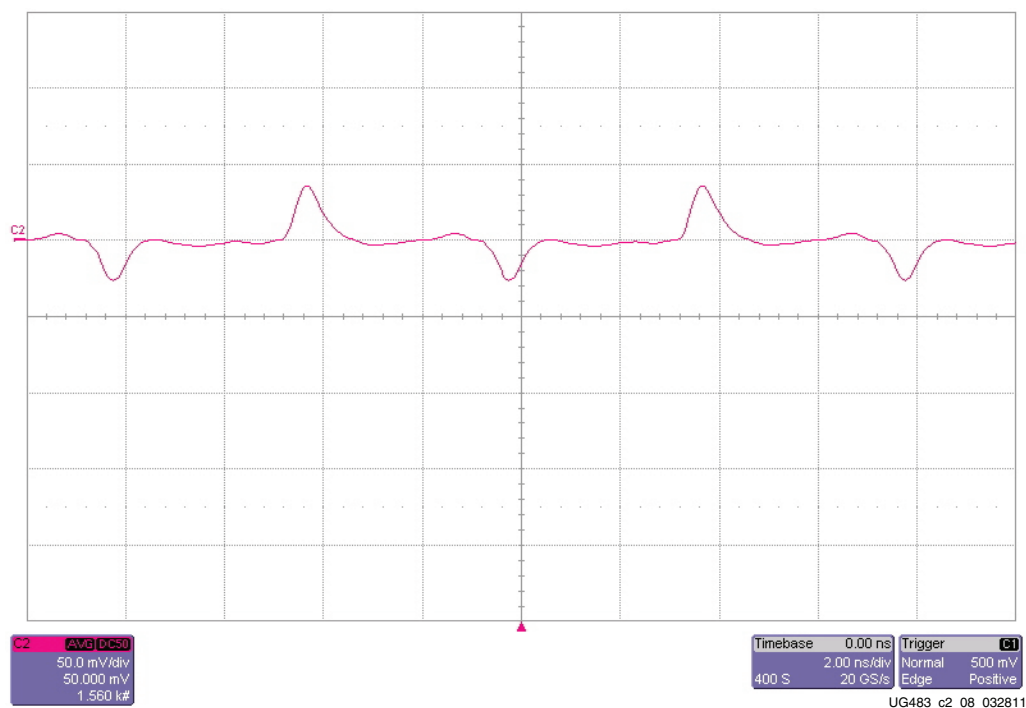


Figure 2-8: Averaged Measurement of  $V_{CC0}$  Supply with Multiple I/O Sending Patterns at 250 Mb/s



Figure 2-9 shows an infinite persistence noise measurement of the same design with a wider variety of I/O activity. Because the infinite persistence measurement catches *all* noise events over a long period, both correlated and non-correlated with the primary aggressor, all power system excursions are shown.

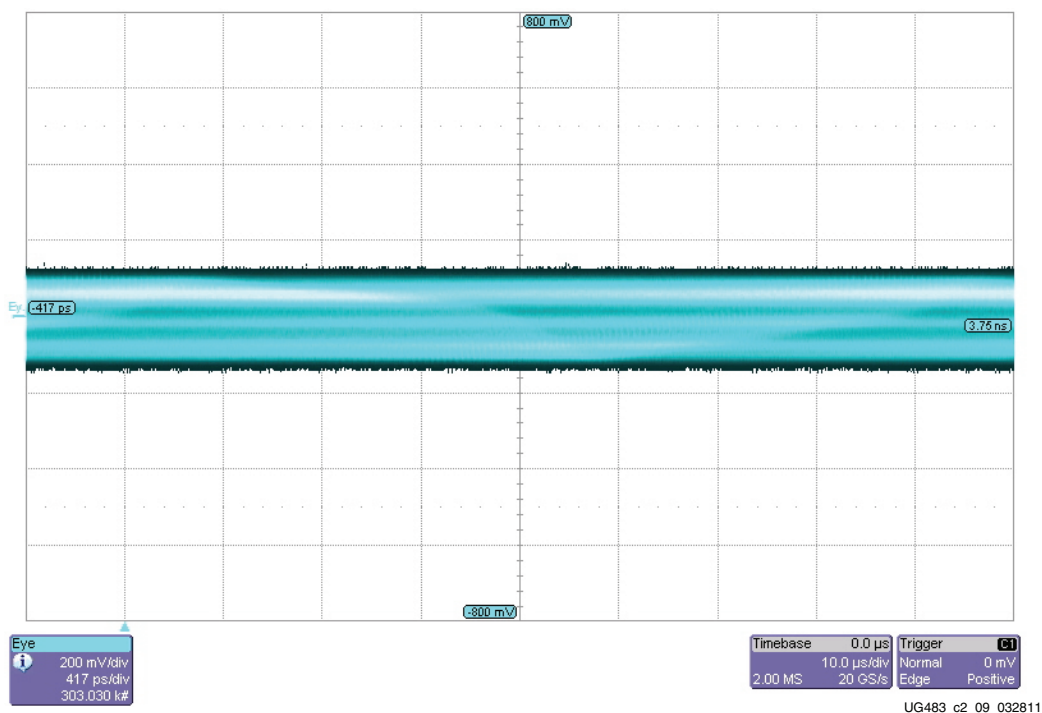


Figure 2-9: Infinite Persistence Measurement of Same Supply

The measurement shown in Figure 2-8 and Figure 2-9 represents the peak-to-peak noise. If the peak-to-peak noise is outside the specified acceptable voltage range, the decoupling network is inadequate or a problem exists in the PCB layout.

## Noise Spectrum Measurements

Having the necessary information to improve the decoupling network requires additional measurements. To determine the frequencies where the noise resides, noise power spectrum measurement is necessary. A spectrum analyzer or a high-bandwidth oscilloscope coupled with FFT math functionality can accomplish this.

The FFT math function can be built into the oscilloscope, however, many of these functions do not have resolution sufficient to give a clear picture of the noise spectrum. Alternatively, a long sequence of time-domain data can be captured from an oscilloscope and converted to frequency domain using MATLAB or other post-processing software supporting FFT. This method has the advantage of showing as much resolution as the user is willing to process. If neither math capacity is available, the noise frequency content can be approximated by visually examining the time-domain waveform and estimating the individual periodicities present in the noise.

A spectrum analyzer is a frequency-domain instrument, showing the frequency content of a voltage signal at its inputs. Using a spectrum analyzer, the user sees the exact frequencies where the PDS is inadequate.



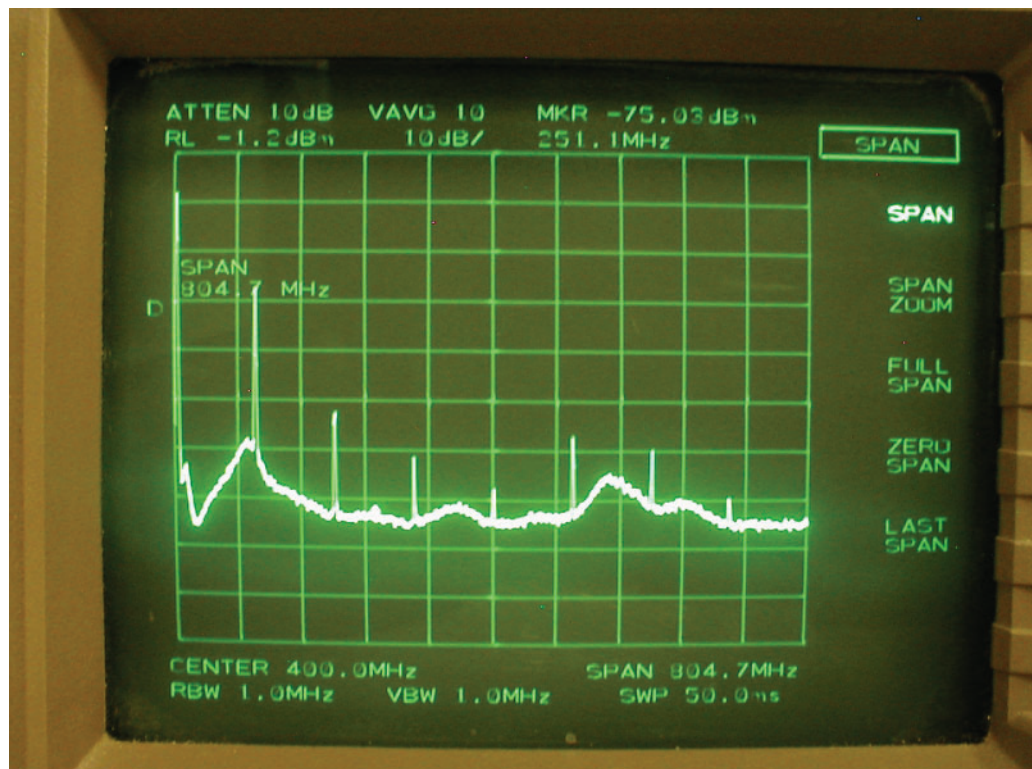
Excessive noise at a certain frequency indicates a frequency where the PDS impedance is too high for the device's transient current demands. Using this information, the designer can modify the PDS to accommodate the transient current at the specific frequency. This is accomplished by either adding capacitors with effective frequencies close to the noise frequency or otherwise lowering the PDS impedance at the critical frequency.

The noise spectrum measurement should be taken in the same manner as the peak-to-peak noise measurement, directly underneath the device, or at a static I/O driven High or Low. A spectrum analyzer takes its measurements using a 50Ω cable instead of an active probe.

- A good method attaches the measurement cable through a coaxial connector tapped into the power and ground planes close to the device. This is *not* available in most cases.
- Another method attaches the measurement cable at the lands of a decoupling capacitor in the vicinity of the device that has been removed. The cable's center conductor and shield are soldered directly to the capacitor lands. Alternatively, a probe station with 50Ω RF probes can be used to touch the decoupling capacitor lands.

To protect the spectrum analyzer's sensitive front-end circuitry, add a DC blocking capacitor or attenuator in line. This isolates the spectrum analyzer from the device supply voltage.

Figure 2-10 is an example of a noise spectrum measurement of the  $V_{CCO}$  power-supply noise, with multiple I/O sending patterns at 100 MHz.



UG483\_c2\_10\_032811

Figure 2-10: Screenshot of Spectrum Analyzer Measurement of  $V_{CCO}$

## Optimum Decoupling Network Design

If a highly optimized PDS is needed, measurements and simulations of a prototype system can inform the PDS design. Using knowledge of the noise spectrum generated by the prototype system along with knowledge of the system's power system impedance, the unique transient current of the design can be determined and accommodated.

To measure the noise spectrum of the design under operating conditions, use either a spectrum analyzer or an oscilloscope with FFT. The power system impedance can be determined either through direct measurement or simulation, or a combination of these two as there are often many variables and unknowns.

Both the noise spectrum and the impedance are functions of frequency. By examining the quotient of these per frequency point, transient current as a function of frequency is computed (Equation 2-7):

$$I(f) = \frac{V(f) \text{ From Spectrum Analyzer}}{Z(f) \text{ From Network Analyzer}} \quad \text{Equation 2-7}$$

Using the data sheet's maximum voltage ripple value, the impedance value needed at all frequencies can be determined. This yields a target impedance as a function of frequency. A specially designed capacitor network can accommodate the specific design's transient current.

## Troubleshooting

In some cases the proper design work is done up-front, but noise problems still exist. This next section describes possible issues and suggested resolution methods.

### Possibility 1: Excessive Noise from Other Devices on the PCB

Sometimes ground and/or power planes are shared among many devices, and noise from an inadequately decoupled device affects the PDS at other devices. Common causes of this noise are:

- RAM interfaces with inherently high-transient current demands resulting either from temporary periodic contention or high-current drivers
- Large ASICs

When unacceptable amounts of noise are measured locally at these devices, the local PDS and the component decoupling networks should be analyzed.

### Possibility 2: Parasitic Inductance of Planes, Vias, or Connecting Traces

Sometimes the decoupling network capacitance is adequate, but there is too much inductance in the path from the capacitors to the FPGA.

Possible causes are:

- Wrong decoupling capacitor connecting-trace geometry or solder-land geometry
- The path from the capacitors to the FPGA is too long  
- and/or -
- A current path in the power vias traverses an exceptionally thick PCB stackup

For inadequate connecting trace geometry and capacitor land geometry, review the loop inductance of the current path. If the vias for a decoupling capacitor are spaced a few

millimeters from the capacitor solder lands on the board, the current loop area is greater than necessary.

To reduce the current loop area, vias should be placed directly against capacitor solder lands. *Never* connect vias to the lands with a section of trace.

Other improvements of geometry are via-in-pad (via under the solder land), not shown, and via-beside-pad (vias straddle the lands instead of being placed at the ends of the lands). Double vias also improve connecting trace geometry and capacitor land geometry.

Exceptionally thick boards (> 3.2 mm or 127 mils) have vias with higher parasitic inductance.

To reduce the parasitic inductance, move critical  $V_{CC}/GND$  plane sandwiches close to the top surface where the FPGA is located, and place the capacitors on the top surface where the FPGA is located.

### Possibility 3: I/O Signals in PCB are Stronger Than Necessary

If noise in the  $V_{CCO}$  PDS is still too high after refining the PDS, the I/O interface slew rate and/or drive strength can be reduced. This applies to both outputs from the FPGA and inputs to the FPGA. In severe cases, excessive overshoot on inputs to the FPGA can reverse-bias the IOB clamp diodes, injecting current into the  $V_{CCO}$  PDS.

If large amounts of noise are present on  $V_{CCO}$ , the drive strength of these interfaces should be decreased, or different termination should be used (on input or output paths).

### Possibility 4: I/O Signal Return Current Traveling in Sub-Optimal Paths

I/O signal return currents can also cause excessive noise in the PDS. For every signal transmitted by a device into the PCB (and eventually into another device), there is an equal and opposite current flowing from the PCB into the device's power/ground system. If a low-impedance return current path is not available, a less optimal, higher impedance path is used. When I/O signal return currents flow over a less optimal path, voltage changes are induced in the PDS, and the signal can be corrupted by crosstalk. This can be improved by ensuring every signal has a closely spaced and fully intact return path.

Methods to correct a sub-optimal return current path:

- Restrict signals to fewer routing layers with verified continuous return current paths.
- Provide low-impedance paths for AC currents to travel between reference planes (high-frequency decoupling capacitors at PCB locations where layer transitions occur).



# SelectIO Signaling

---

The 7 series FPGA SelectIO resources are the general-purpose I/O and its various settings. With numerous I/O standards and hundreds of variants within these standards, these SelectIO resources offer a flexible array of choices for designing I/O interfaces.

This chapter provides some strategies for choosing I/O standard, topography, and termination, and offers guidance on simulation and measurement for more detailed decision making and verification. In many cases, higher-level aspects of the system (other device choices or standards support) define the I/O interfaces to be used. In cases where such constraints are not defined, it is up to the system designer to choose I/O interface standards and optimize them according to the purpose of the system.

This chapter contains the following sections:

- [Interface Types](#)
- [Single-Ended Signaling](#)

## Interface Types

To better address the specifics of the various interface types, it is necessary to first break interfaces into categories. Two relevant divisions are made:

- Single-Ended interfaces versus Differential interfaces
- Single Data Rate (SDR) interfaces versus Double Data Rate (DDR) interfaces

### Single-Ended versus Differential Interfaces

Traditional digital logic uses single-ended signaling – a convention that transmits a signal and assumes a GND common to the driver and receiver. In single-ended interfaces, a signal's assertion (whether it is High or Low) is based on its voltage level relative to a fixed voltage threshold that is referenced to GND. When the voltage of the signal is higher than the  $V_{IH}$  threshold, the state is considered High. When the voltage of the signal is lower than the  $V_{IL}$  threshold, the state is considered Low. TTL is one common example of a single-ended I/O standard.

To reach higher interface speeds and increase noise margin, some single-ended I/O standards rely on a precise dedicated local reference voltage other than GND. HSTL and SSTL are examples of I/O standards that rely on a  $V_{REF}$  to resolve logic levels.  $V_{REF}$  can be thought of as a fixed comparator input.

Higher-performance interfaces typically make use of differential signaling – a convention that transmits two complementary signals referenced to one another. In differential interfaces, a signal's assertion (whether it is High or Low) is based on the relative voltage levels of the two complementary signals. When the voltage of the P signal is higher than

the voltage of the N signal, the state is considered High. When the voltage of the N signal is higher than the voltage of the P signal, the state is considered Low. Typically the P and N signals have similar swing, and have a common-mode voltage above GND (although this is not always the case). LVDS is one common example of a differential I/O standard.

## SDR versus DDR Interfaces

The difference between Single Data Rate (SDR) and Double Data Rate (DDR) interfaces has to do with the relationship of the data signals of a bus to the clock signal of that bus. In SDR systems, data is only registered at the input flip-flops of a receiving device on either the rising *or* the falling edge of the clock. One full clock period is equivalent to one bit time. In DDR systems, data is registered at the input flip-flops of a receiving device on both the rising *and* falling edges of the clock. One full clock period is equivalent to two bit times. The distinction of SDR and DDR has nothing to do with whether the I/O standard carrying the signals is single-ended or differential. A single-ended interface can be SDR or DDR, and a differential interface can also be SDR or DDR.

## Single-Ended Signaling

A variety of single-ended I/O standards are available in the 7 series FPGA I/O. For a complete list of supported I/O standards and detailed information about each one, refer to the “SelectIO Resources” chapter of [UG471, 7 Series FPGAs SelectIO Resources User Guide](#). Tables at the end of this chapter summarize for each supported I/O standard which ones support DRIVE and SLEW attributes, bidirectional buffers, and the DCI options. It also describes which I/O standards are supported in the high-performance (HP) and high-range (HR) I/O banks.

## Modes and Attributes

Some I/O standards can be used only in unidirectional mode, while some can be used in bidirectional mode or unidirectional mode.

Some I/O standards have attributes to control drive strength and slew rate, as well as the presence of weak pull-up or pull-down and weak-keeper circuits (not intended for use as parallel termination). Drive strength and slew rate can be used to tune an interface for adequate speed while not overdriving the signals. Weak pull-ups, weak pull-downs, and weak keepers can be used to ensure a known or steady level on a floating or 3-stated signal. The “SelectIO Resources” chapter of [UG471, 7 Series FPGAs SelectIO Resources User Guide](#) describes which standards support these attributes. Refer to this user guide for more information.

LVC MOS, when set to 6 mA DRIVE and FAST slew, has an approximate output impedance close to 50Ω, allowing it to be used as a crude approximation of a controlled-impedance driver. The impedance match of the weak driver to the transmission line is only approximate and varies with voltage and temperature. LVDCI and HSLVDCI, true controlled-impedance drivers, are adaptive, maintain a much closer impedance match, and remain constant over voltage and temperature.

## Input Thresholds

The input circuitry of the single-ended standards fall into two categories: those with fixed input thresholds and those with input thresholds set by the  $V_{REF}$  voltage. The use of  $V_{REF}$  has three advantages:



- It allows for tighter control of input threshold levels
- It removes dependence on die GND for the threshold reference
- It allows for input thresholds to be closer together, which reduces the need for a large voltage swing of the signal at the input receiver

Two 1.8V I/O standards that illustrate this are LVCMOS18 and SSTL18 Class 1. The thresholds for 1.8V LVCMOS are set at 0.63V and 1.17V (necessitating that the signal at the receiver swing a full 540 mV at minimum to make a logic transition). The thresholds for SSTL18 Class 1 are set at  $V_{REF} - 0.125V$  and  $V_{REF} + 0.125V$ , or for a nominal  $V_{REF}$  of 0.9V, set at 0.775V and 1.025V (necessitating that the signal at the receiver only swing 250 mV at minimum to make a logic transition). This smaller required swing allows for higher frequency of operation in the overall link. A smaller swing at the driver means reduced DC power is required with less transient current. A historical drawback to the use of  $V_{REF}$  was that the semi-dedicated  $V_{REF}$  pins of the bank could not be used as I/Os whenever an I/O standard was used in a bank that required the  $V_{REF}$  supply. However, with the 7 series devices, the reference voltage can either be provided using the semi-dedicated  $V_{REF}$  pins, or optionally generated internally using the Internal  $V_{REF}$  feature. See [UG471, 7 Series FPGAs SelectIO User Guide](#) for more details on Internal  $V_{REF}$ . For more information on  $V_{REF}$  decoupling and decoupling of all other supplies, see [Chapter 2, Power Distribution System](#).

## Topographies and Termination

Topography generally refers to the arrangement of drivers, receivers, interconnect and terminations in an interface. The techniques used in unidirectional topographies are different from those used in bidirectional topographies, so these are treated separately.

The SelectIO standards can be used in countless topographies depending on the requirements of the system. SelectIO drivers and receivers adhering to a standard (SSTL, LVCMOS, etc.) either can be used according to the letter of the standard (published by a standards body such as EIA/TIA or JEDEC) or they can be mixed and matched with drivers or receivers from another standard or hybrid I/O. An I/O standard specification might define something as limited as the  $V_{IL}$  and  $V_{IH}$  of the receiver, or it might define every aspect of the interface, including driver impedance and slew rate, PCB trace length and topography, value and position of passive termination, the maximum input capacitance of a receiving device, and even the maximum number of receivers.

It is up to the designer to apply the standard in question to the system in which it is working. There are many decisions to make with respect to topographies and termination, which determine the signal integrity of the interface. It is of utmost importance that the signal integrity of each interface be verified through both simulation and measurement.

Termination generally refers to impedance-matching or impedance-compensating devices that are used to maintain signal integrity in an interface. While many types of elements can be used as *terminators* (such as, resistors, capacitors, diodes), this discussion is limited to resistive termination. In general, capacitor and diode termination techniques are more complicated.

## Unidirectional Topographies and Termination

The two basic subsets of unidirectional topographies are point-to-point and multi-drop. A point-to-point topography has one driver and one receiver, while a multi-drop topography has one driver and many receivers. Whether or not a topography is point-to-point or multi-drop defines important aspects of the interface that determine which termination strategies are appropriate and which are not.

## Unidirectional Point-to-Point Topographies

The simplest unidirectional topography is point-to-point. That is, there is one driver and one receiver. Termination, if present, can consist of parallel termination at the receiver (Figure 3-1), series termination at the driver (Figure 3-2), or a controlled-impedance driver (Figure 3-3 and Figure 3-4). Always use IBIS simulation to determine the optimal resistor values,  $V_{TT}$  voltage level, and VRN/VRP reference resistors for these terminations.

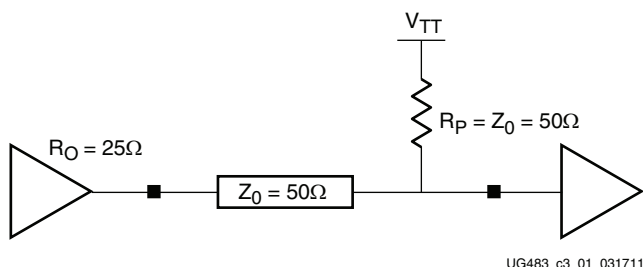


Figure 3-1: **Parallel-Terminated Unidirectional, Point-to-Point Topography**

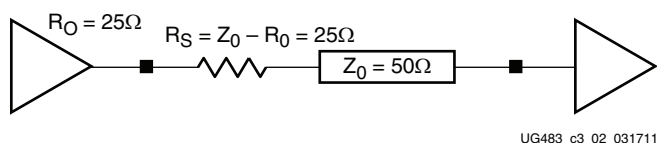


Figure 3-2: **Series-Terminated Unidirectional, Point-to-Point Topography**

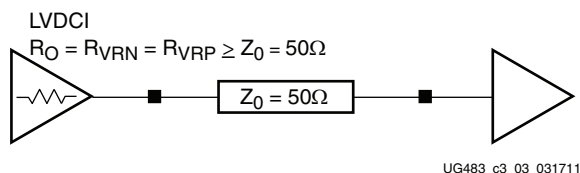


Figure 3-3: **DCI-Controlled Impedance Driver Unidirectional, Point-to-Point Topography**

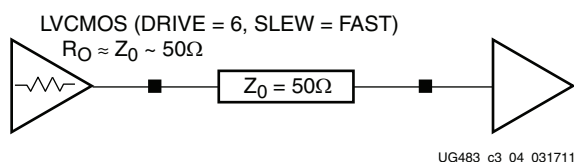


Figure 3-4: **"Weak Driver" Unidirectional, Point-to-Point Topography**

In general, parallel resistive termination ( $R_P$ ) has a value equal to the characteristic impedance ( $Z_0$ ) of the transmission line it is terminating. Series resistive terminations ( $R_S$ ) have a value equal to the characteristic impedance of the transmission line ( $Z_0$ ) minus the output impedance of the driver ( $R_O$ ) to which they are connected. Controlled-impedance drivers are tuned such that the driver output impedance ( $R_O$ ) is equal to the characteristic impedance ( $Z_0$ ) of the transmission line it is terminating.

Assuming transmission lines with 50Ω characteristic impedance and a driver output impedance ( $R_O$ ) of 25Ω, a 25Ω series termination (Figure 3-2) or a 50Ω parallel termination (Figure 3-1) is appropriate. Controlled-impedance drivers, whether



implemented with DCI or with weak LVCMOS drivers, should be sized to have an output impedance ( $R_O$ ) of  $50\Omega$ . This corresponds to VRN and VRP resistors equal to  $50\Omega$  for DCI. Weak LVCMOS drivers of 6 mA to 8 mA drive strength have an output impedance approximately equal to  $50\Omega$  (Figure 3-3).

Typically, parallel terminations have best performance when  $V_{TT}$  (the voltage source connected to the parallel termination resistor) is equal to half of the signaling voltage. For 2.5V signals ( $V_{CCO} = 2.5V$ ),  $V_{TT}$  is ideally 1.25V. In cases where this voltage is not available, it is possible to use a Thevenin parallel termination. Thevenin parallel termination consists of a voltage divider with a parallel equivalent resistance ( $R_{PEQ}$ ) equal to the characteristic impedance of the transmission line ( $50\Omega$  in most cases). The divided voltage point is designed to be at  $V_{TT}$ . Figure 3-5 illustrates a Thevenin parallel termination powered from 2.5V  $V_{CCO}$ , made up of two  $100\Omega$  resistors, resulting in a  $V_{TT}$  of 1.25V and a parallel equivalent resistance ( $R_{PEQ}$ ) of  $50\Omega$ .

Parallel termination can be less desirable than series termination or controlled-impedance drivers because it dissipates more power. This trade-off must be weighed against other trade-offs to determine the optimum termination topography for an interface.

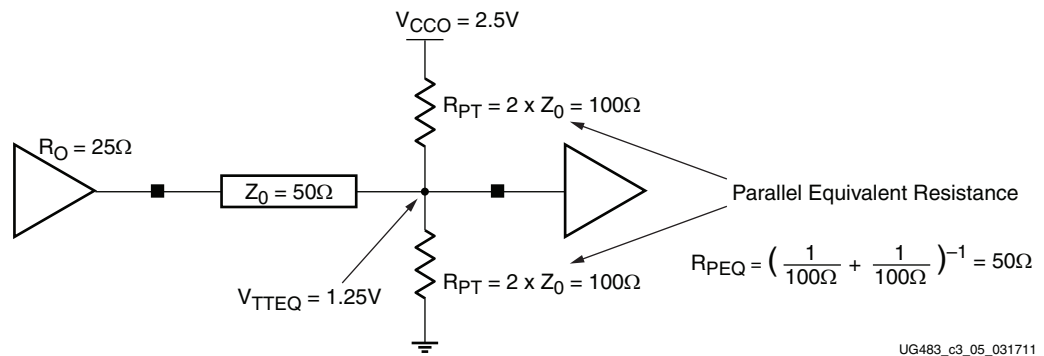


Figure 3-5: Thevenin Parallel Termination

Table 3-1 lists example I/O interface types that can be used with the unidirectional point-to-point topography.

Table 3-1: Example I/O Interface Type for Unidirectional Point-to-Point Topographies

LVTTL
LVCMOS
LVDCI
SSTL Class I
HSTL Class I

LVTTL and LVCMOS do not specify any canonical termination method. Series termination at the driver or parallel termination at the receiver are both appropriate considerations.

LVDCI implicitly uses controlled-impedance driver termination. No form of termination is needed at the receiver.

Every I/O standard can have different requirements for termination techniques. In some cases the specification for the I/O standard can rigidly define the termination topology. Other standards might not have any hard requirements, but rather might simply provide

examples of termination topologies. An example of a standard with specific termination requirements is HSTL. HSTL Class I is a unidirectional I/O standard that recommends a parallel termination at the receiver. In the case of HSTL Class I, the termination voltage  $V_{TT}$  is defined as half of the supply voltage  $V_{CC}$ . The designer can ultimately elect either not to use termination at all or to use a different termination, such as series termination at the driver. There are a number of reasons why this selection might be advantageous in a given system. It is up to the designer to verify through simulation and measurement that the signal integrity at the receiver is adequate.

The SSTL standards tend to not have rigid requirements for termination topology. Rather, the JEDEC specifications provide example termination techniques that tend to be the commonly used topographies. The “SelectIO Resources” chapter of [UG471, 7 Series FPGAs SelectIO Resources User Guide](#) provides example termination techniques for each of the I/O standards, including the SSTL standards, for the purpose of providing a good starting point for consideration. Similar to HSTL, it is ultimately up to the designer to verify through simulation and measurement that the signal integrity at the receiver is adequate.

### Unidirectional Multi-Drop Topographies

In more complex topographies, a single driver can drive multiple receivers. The receivers represent loads that must be fed by individual transmission line stubs. From a signal integrity standpoint, the best topography to use in this case is a single long transmission line with the driver at one end and parallel termination at the other, with receivers connected to the main trace by short stubs in between. This type of topography is often referred to as a *flyby multi-drop* topography.

There are two critical aspects of this topography. The first is the presence of a single parallel termination at the far end of the transmission line. Series termination at the driver or a controlled impedance driver must *never* be used. Parallel termination is the only applicable termination type for this topography. The second critical aspect is the length of the connecting stubs at each receiver. These must remain short: no more than a fraction of a signal rise time in length. With a typical signal rise time of 600 ps, a stub no longer than  $700 \text{ ps} / 4 = 150 \text{ ps}$ , or 0.9 inches (22.86 mm) should be used. As the stubs become longer, they present a larger impedance discontinuity to the signal travelling down the transmission line, and can support significant reflections. These impedance discontinuities corrupt the signal. With increasing numbers of loads and increasing length of stubs, the signal is corrupted to the point where it is no longer usable.

Star topographies are not recommended. The constraints involved in designing a star topography with good signal integrity are beyond the scope of this document.

As stated in [Unidirectional Point-to-Point Topographies](#), ideal parallel resistive termination has a value equal to the characteristic impedance of the transmission line it is terminating. The best performance is achieved when  $V_{TT}$  is equal to half of the signaling voltage, and when this voltage is not available, a Thevenin parallel termination is recommended, as defined in the previous section.

[Figure 3-6](#) illustrates a Thevenin parallel termination powered from  $V_{CC0}$ , made up of two  $100\Omega$  resistors, resulting in a  $V_{TT}$  of  $V_{CC0}/2$  and a parallel equivalent resistance of  $50\Omega$ . This figure shows a topography with one driver (an LVCMOS driver) and four receivers. The driver is on the left side, the receivers are spaced at interim points across the  $50\Omega$  transmission line, and the Thevenin parallel termination of two  $100\Omega$  resistors is on the right side.

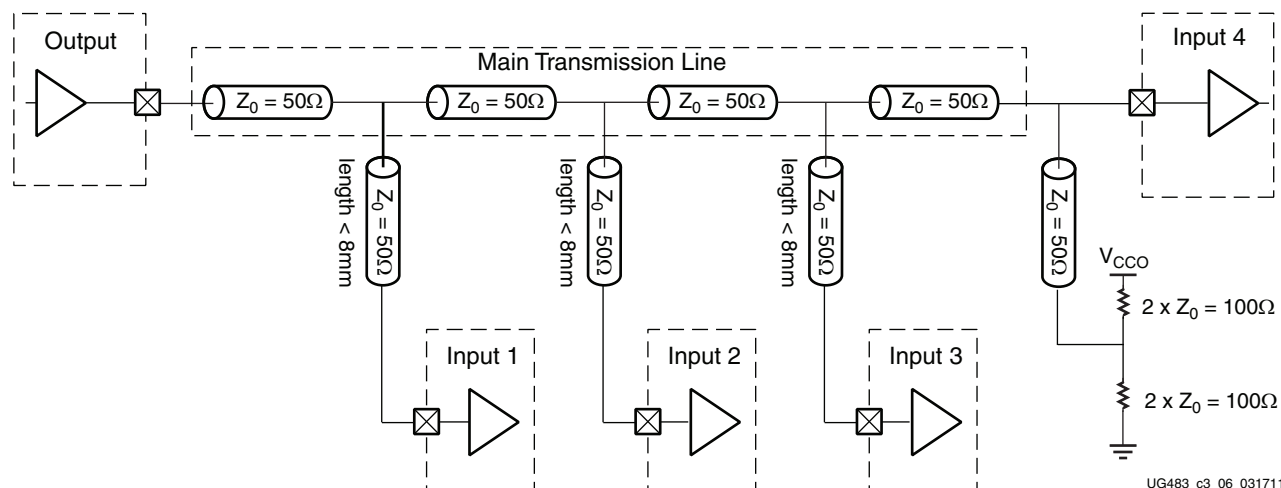


Figure 3-6: Basic Multi-Drop Topography

The main transmission line should be kept as short as possible. Lengths up to 20 inches or more are practical for most I/O standards as long as precise trace impedance is maintained and crosstalk sources are avoided. The lengths of interim segments of the main transmission line need not be equal. Their relative lengths can be arbitrary. Receivers at different points along the main transmission line receive the signal with varying amounts of delay, but all signal rise times are similar.

*Stubs stretching from the main transmission line to the individual receivers must be kept as short as possible.* The longer these stubs become, the more corrupted the received waveforms are. Simulation and measurement are required to assess signal integrity at the individual receivers.

Table 3-2 lists example I/O interface types that can be used with the unidirectional multi-drop topography.

Table 3-2: Example I/O Interface Types for Unidirectional Multi-Drop I/O Topographies

LVTTL
LVC MOS
HSTL
SSTL

LVTTL and LVC MOS do not specify any canonical termination method. Parallel termination at the end of the long t-line is an appropriate termination method.

## Bidirectional Topography and Termination

The two basic subsets of bidirectional topographies are point-to-point and multi-point. A point-to-point topography has two transceivers (driver and receiver sharing one device pin), while a multi-point topography can have many transceivers. Whether or not a topography is point-to-point or multi-point defines important aspects of the interface that determine which termination strategies are appropriate and which are not.

## Bidirectional Point-to-Point Topographies

The simplest bidirectional topography is point to point. That is, there are two transceivers connected by a transmission line. Because bidirectional interfaces need to operate equally well in both directions, symmetry of the topography is desirable. While asymmetrical topographies can be designed with reasonably good signal integrity, the easiest way to ensure good signal integrity is to keep the topography symmetrical. Thus any termination used on one side of the link should also be used on the other side of the link. Series termination (Figure 3-8) is rarely appropriate for bidirectional interfaces as incoming signals are attenuated by the series resistor of the receiving transceiver. Parallel termination (Figure 3-7) almost always achieves better signal levels at both receivers. Controlled-impedance drivers, whether crudely controlled in the form of a weak LVCMOS driver or adaptively controlled in the form of LVDCI or HSLVDCI, also can have good results as shown in Figure 3-9, Figure 3-10, and Figure 3-11 (implemented with a low-drive strength LVCMOS driver). Always use IBIS simulation to determine the optimal termination resistor value,  $V_{TT}$  voltage level and VRN/VRP reference resistor values for these terminations.

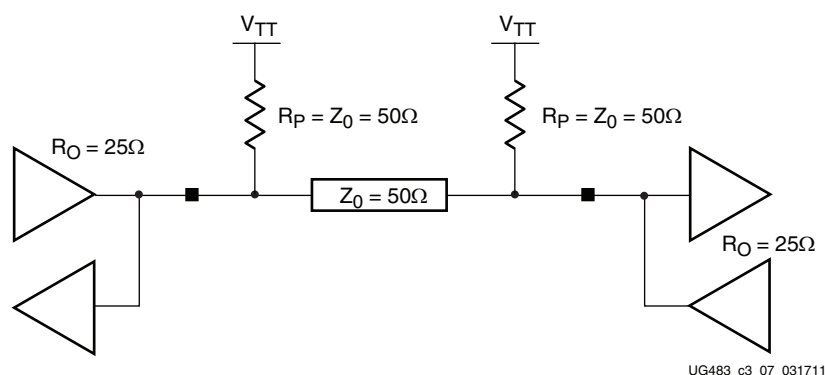


Figure 3-7: Parallel Terminated Bidirectional Point-to-Point Topography

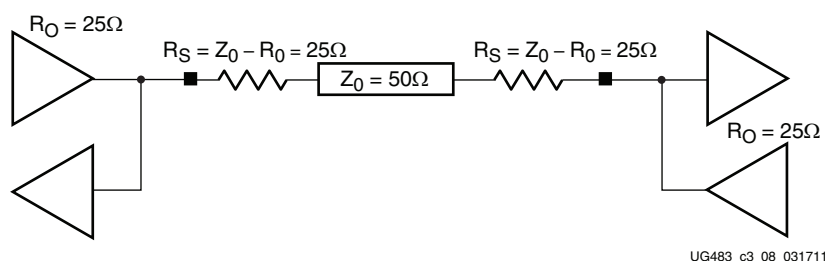
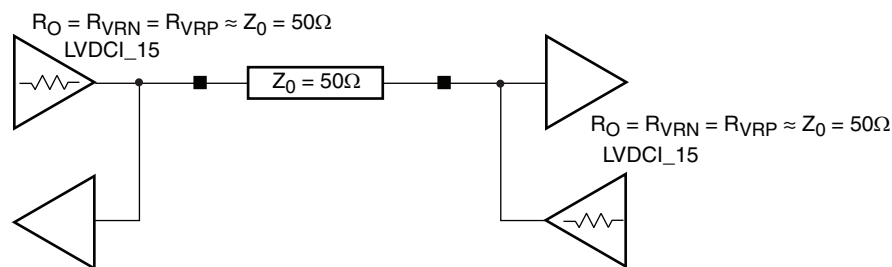
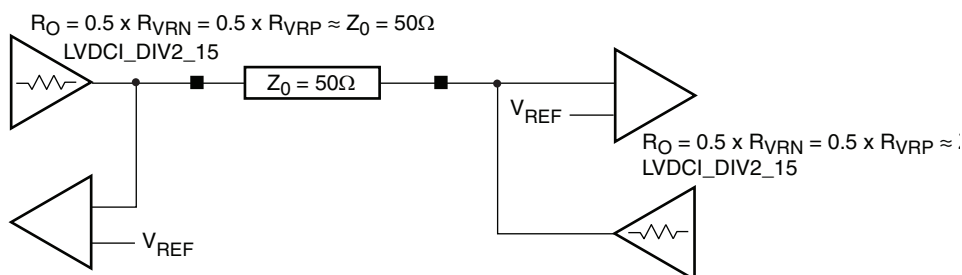


Figure 3-8: Series Terminated Bidirectional Point-to-Point Topography:  
Not Recommended



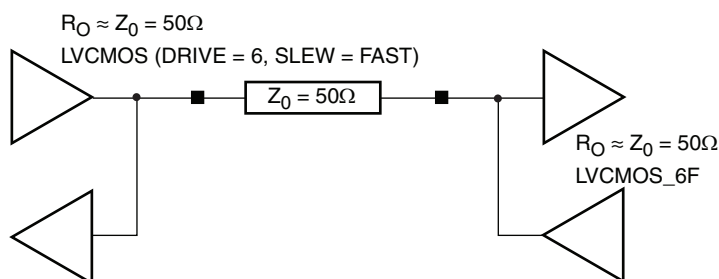
UG483\_c3\_09\_032411

Figure 3-9: DCI Controlled Impedance Bidirectional Point-to-Point Topography



UG483\_c3\_10\_032411

Figure 3-10: HSLVDCI Controlled Impedance Driver Bidirectional Point-to-Point Topography



UG483\_c3\_11\_031711

Figure 3-11: "Weak Driver" Bidirectional Point-to-Point Topography

In general, parallel resistive termination ( $R_p$ ) has a value equal to the characteristic impedance  $Z_0$  of the transmission line it is terminating. Some interfaces, such as DDR2 memory interfaces, use  $75\Omega$  termination resistors instead of  $50\Omega$  in an effort to open the data eye. In this case, the trade-off is eye height against a small amount of signal reflection from the impedance discontinuity. Controlled-impedance drivers are typically tuned such that the driver output impedance ( $R_O$ ) is equal to the characteristic impedance ( $Z_0$ ) of the transmission line it is terminating.

Assuming transmission lines with  $50\Omega$  characteristic impedance and a driver output impedance of  $25\Omega$ ,  $50\Omega$  parallel terminations are appropriate (Figure 3-7). Controlled-impedance drivers, whether implemented with DCI or with weak LVCMOS drivers, should be sized to have an output impedance ( $R_O$ ) of  $50\Omega$ . An example of the use of a controlled-impedance driver would be the LVDCI\_15 I/O standard. By using  $50\Omega$  external precision resistors placed on the VRN and VRP pins for that bank, the resulting controlled output impedance for that bank would be  $50\Omega$ . If  $100\Omega$  resistors were already required on the VRN and VRP pins (for the purpose of creating a Thevenin-equivalent split

termination circuit equal to  $50\Omega$ ), and a  $50\Omega$  controlled impedance driver was required in the same bank, this could be accomplished by using the “DIV2” versions of the drivers, such as LVDCI\_DIV2\_15 (Figure 3-9 and Figure 3-10). Weak LVCMOS drivers of 6 mA to 8 mA drive strength have an output impedance approximately equal to  $50\Omega$  (Figure 3-11).

Parallel terminations have the best performance when  $V_{TT}$  (the voltage source connected to the parallel termination resistor) is equal to half of the signaling voltage, since this is typically the center voltage of the data eye. For 2.5V signals ( $V_{CCO} = 2.5V$ ),  $V_{TT}$  is ideally 1.25V. In cases where this voltage is not available, it is advisable to use a Thevenin parallel termination. Thevenin parallel termination consists of a voltage divider with a parallel resistance equal to the characteristic impedance of the transmission line ( $50\Omega$  in most cases). The divided voltage point is designed to be at  $V_{TT}$ . Figure 3-12 illustrates a Thevenin parallel termination powered from 2.5V  $V_{CCO}$ , made up of two  $100\Omega$  resistors, resulting in a  $V_{TT}$  of 1.25V and a parallel equivalent resistance ( $R_{PEQ}$ ) of  $50\Omega$ .

Parallel termination can be less desirable than series termination or controlled-impedance drivers because it dissipates more power. This trade-off must be weighed against other trade-offs to determine the optimum termination topography for an interface.

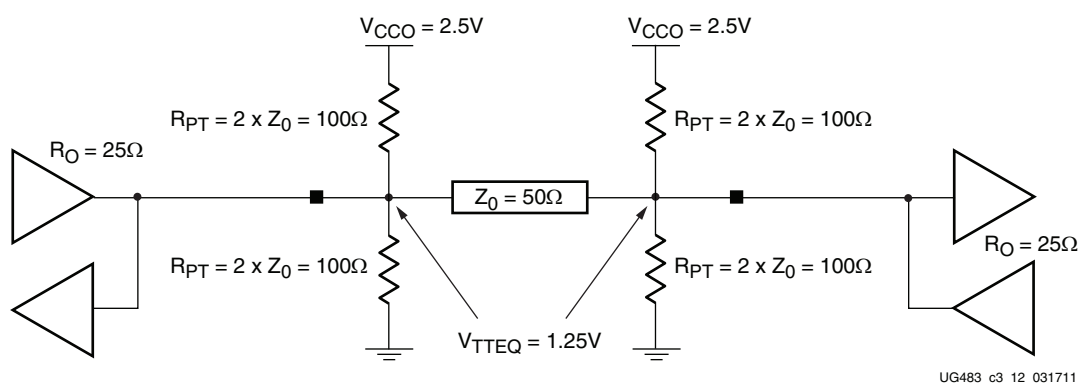


Figure 3-12: Thevenin Parallel Termination (Bidirectional Point-to-Point Topography)

Table 3-3 lists example I/O interface types that can be used with the bidirectional point-to-point topography.

Table 3-3: Example I/O Interface Types for Bidirectional Point-to-Point I/O Topographies

LVTTL
LVCMOS
LVDCI
HSLVDCI
SSTL15
SSTL15 DCI
SSTL18 CLASS II
SSTL18 CLASS II DCI
HSTL CLASS II
HSTL CLASS II DCI

LVTTL and LVCMOS do not specify any canonical termination method. Series termination is not recommended for bidirectional interfaces. Parallel termination and weak drivers, however, are both appropriate.

LVDCI and HSLVDCI both implicitly use controlled-impedance driver termination.

HSTL Class II specifies parallel termination at both transceivers. The termination voltage  $V_{TT}$  is defined as half of the supply voltage  $V_{CCO}$ . The designer can elect either not to use termination at all or to use a different termination. It is up to the designer to verify through simulation and measurement that the signal integrity at the receiver is adequate.

The JEDEC specifications for SSTL provide examples of both series termination and parallel termination. The termination voltage  $V_{TT}$  is defined as half of the supply voltage  $V_{CCO}$ . While the specification document provides examples depicting series termination at the drivers, it is important to note that the purpose of this is to attempt to match the impedance of the driver with that of the transmission line. Because the 7 series FPGA SSTL drivers target to have output impedances close to  $40\text{--}50\Omega$ , better signal integrity can be achieved without any external source-series termination. When possible, it is a better starting point to consider the use of the 3-state DCI I/O standards ("T\_DCI"), which provide internal parallel termination resistors that are only present when the output buffer is in 3-state. It is up to the designer to carefully choose the I/O standard(s) at the 7 series device, drive strengths, and on-die termination (ODT) options at the other device(s) in the interface (usually DRAM ICs) and termination topography through careful simulation and measurement. See [UG471](#), *7 Series FPGAs SelectIO User Guide* for more details on the available I/O standards and options.

## Bidirectional Multi-Point Topographies

In more complex topographies, any transceiver in a multi-point bus can transmit to all other transceivers. Usually these topographies can only run at very slow clock rates because they only support very slow signal rise times (10 ns to 50 ns). While useful in some situations, the drawbacks usually outweigh the benefits. The constraints involved in designing these topographies with good signal integrity are beyond the scope of this document.





## PCB Materials and Traces

---

The choice of transmission media, whether PCB materials or cable type, can have a large impact on system performance. Although any transmission medium is lossy at gigahertz frequencies, this chapter provides some guidelines on managing signal attenuation so as to obtain optimal performance for a given application.

### How Fast is Fast?

Signal edges contain frequency components called harmonics. Each harmonic is a multiple of the signal frequency and has significant amplitude up to a frequency determined by [Equation 4-1](#):

$$f \approx 0.35 / T \quad \text{Equation 4-1}$$

Where:

$f$  = Frequency in GHz

$T$  = The smaller of signal rise ( $T_r$ ) or fall ( $T_f$ ) time in ns

Because dielectric losses in a PCB are frequency dependent, a bandwidth of concern must be determined to find the total loss of the PCB. Frequencies must start at the operation frequency and extend to the frequency in [Equation 4-1](#). For example, a 10 Gb/s signal with a 10 ps rise time has a bandwidth from 10 GHz to 35 GHz.

### Dielectric Losses

The amount of signal energy lost into the dielectric is a function of the materials characteristics. Some parameters used to describe the material include relative permittivity  $\epsilon_r$  (also known as the dielectric constant) and loss tangent. Skin effect is also a contributor to energy loss at line speeds in the gigahertz range.

#### Relative Permittivity

Relative permittivity is a measure of the effect of the dielectric on the capacitance of a conductor. The higher the relative permittivity, the slower a signal travels on a trace and the lower the impedance of a given trace geometry. A lower  $\epsilon_r$  is almost always preferred.

Although the relative permittivity varies with frequency in all materials, FR4 exhibits wide variations in  $\epsilon_r$  with frequency. Because  $\epsilon_r$  affects impedance directly, FR4 traces can have a spread of impedance values with increasing frequency. While this spread can be insignificant at 1.125 Gb/s, it can be a concern at 10 Gb/s operation.

## Loss Tangent

Loss tangent is a measure of how much electromagnetic energy is lost to the dielectric as it propagates down a transmission line. A lower loss tangent allows more energy to reach its destination with less signal attenuation.

As frequency increases, the magnitude of energy loss increases as well, causing the highest frequency harmonics in the signal edge to suffer the most attenuation. This appears as a degradation in the rise and fall times.

## Skin Effect and Resistive Losses

The skin effect is the tendency for current to flow preferentially near the outer surface of a conductor. This is mainly due to the magnetic fields in higher frequency signals pushing current flow in the perpendicular direction towards the perimeter of the conductor.

As current density near the surface increases, the effective cross-sectional area through which current flows decreases. Resistance increases because the effective cross-sectional area of the conductor is now smaller. Because this skin effect is more pronounced as frequency increases, resistive losses increase with signaling rates.

Resistive losses have a similar effect on the signal as loss tangent. Rise and fall times increase due to the decreased amplitude of the higher harmonics, with the highest frequency harmonics being most affected. In the case of 10 Gb/s signals, even the fundamental frequency can be attenuated to some degree when using FR4.

For example, an 8 mil wide trace at 1 MHz has a resistance on the order of  $0.06\Omega/\text{inch}$ , while the same trace at 10 Gb/s has a resistance of just over  $1\Omega/\text{inch}$ . Given a 10 inch trace and 1.6V voltage swing, a voltage drop of 160 mV occurs from resistive losses of the fundamental frequency, not including the losses in the harmonics and dielectric loss.

## Choosing the Substrate Material

The goal in material selection is to optimize both performance and cost for a particular application.

FR4, the most common PCB substrate material, provides good performance with careful system design. For long trace lengths or high signaling rates, a more expensive substrate material with lower dielectric loss must be used.

Substrates, such as Nelco, have lower dielectric loss and exhibit significantly less attenuation in the gigahertz range, thus increasing the maximum bandwidth of PCBs. At 3.125 Gb/s, the advantages of Nelco over FR4 are added voltage swing margin and longer trace lengths. At 10 Gb/s, a low-loss dielectric like Nelco is necessary unless high-speed traces are kept very short.

The choice of substrate material depends on the total length of the high-speed trace and also the signaling rate.

What-if analysis can be done in HSPICE simulation to evaluate various substrate materials. By varying the dielectric constant, loss tangent, and other parameters of the PCB substrate material. The impact on eye quality can be simulated to justify the use of higher cost materials. The impact of other parameters such as copper thickness can also be explored.

## Traces

### Trace Geometry

For any trace, its characteristic impedance is dependent on its stackup geometry as well as the trace geometry. In the case of differential traces, the inductive and capacitive coupling between the tightly coupled pair also determines the characteristic impedance of the traces.

The impedance of a trace is determined by its inductive and capacitive coupling to nearby conductors. For example, these conductors can be planes, vias, pads, connectors, and other traces, including the other closely coupled trace in a differential pair. The substrate properties, conductor properties, flux linkage area, and distance to a nearby conductor determine the amount of coupling and hence, the contribution to the final impedance.

2D field solvers are necessary in resolving these complex interactions and contribute to the calculation of the final impedance of the trace. They are also a useful tool to verify existing trace geometries.

Wider traces create a larger cross-sectional area for current to flow and reduce resistive losses in high-speed interfaces. Use the widest traces that space constraints allow. Because trace width tolerances are expressed in absolute terms, a wider trace also minimizes the percentage variation of the manufactured trace, resulting in tighter impedance control along the length of the transmission line.

Sometimes, striplines are preferred over microstrips because the reference planes on both sides of the trace provide radiation shielding. Microstrips are shielded on only one side (by the reference plane) because they run on the top-most or bottom-most layers, leaving the other side exposed to the environment.

For best results, the use of a 2D or 3D field solver is recommended for verification.

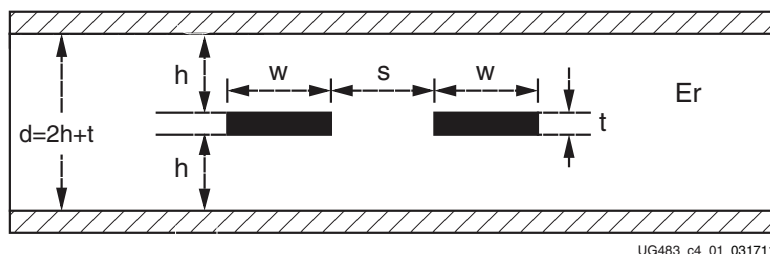
### Trace Characteristic Impedance Design for High-Speed Transceivers

Because the transceivers use differential signaling, the most useful trace configurations are differential edge-coupled stripline and differential microstrip. While some backplanes use the differential broadside-coupled stripline configuration, it is not recommended for 10 Gb/s operation, because the P and N vias are asymmetrical and introduce common-mode non-idealities.

With few exceptions,  $50\Omega$  characteristic impedance ( $Z_0$ ) is used for transmission lines in the channel. In general, when the width/spacing (W/S) ratio is greater than 0.4 (8 mil wide traces with 20 mil separation), coupling between the P and N signals affects the trace impedance. In this case, the differential traces must be designed to have an odd mode impedance ( $Z_{0O}$ ) of  $50\Omega$ , resulting in a differential impedance ( $Z_{DIFF}$ ) of  $100\Omega$ , because  $Z_{DIFF} = 2 \times Z_{0O}$ .

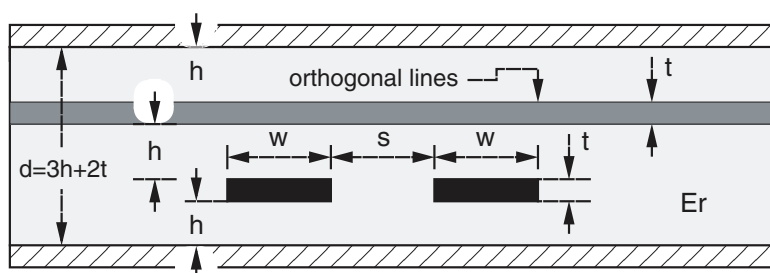
The same W/S ratio also must be less than 0.8, otherwise strong coupling between the traces requires narrower, lossier traces for a  $Z_{0O}$  of  $50\Omega$ . To clarify, with  $Z_{0O}$  at  $50\Omega$ , an even mode impedance ( $Z_{0E}$ ) of  $60\Omega$  or below is desired.

Figure 4-1 through Figure 4-4 show example cross sections of differential structures.



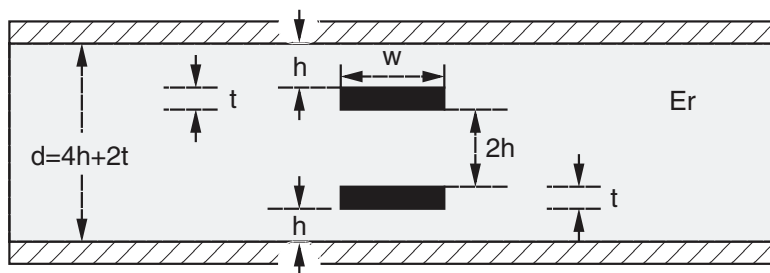
UG483\_c4\_01\_031711

Figure 4-1: Differential Edge-Coupled Centered Stripline



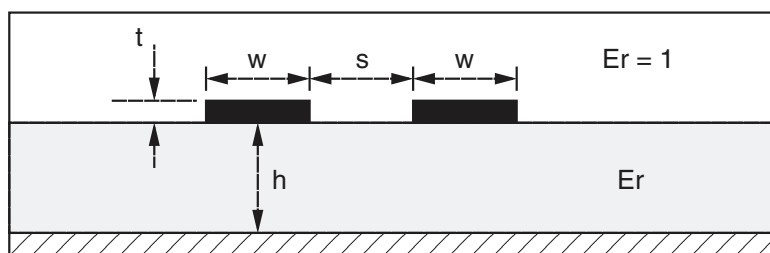
UG483\_c4\_02\_031711

Figure 4-2: Differential Edge-Coupled Offset Stripline



UG483\_c4\_03\_031711

Figure 4-3: Centered Broadside-Coupled Stripline



UG483\_c4\_04\_031711

Figure 4-4: Differential Microstrip

A good PCB manufacturer understands controlled impedance and allows fine adjustments for line widths to produce a  $Z_{0O}$  of  $50\Omega$ . The PCB manufacturer also provides the parameters necessary for the specific PCB layout. Some parameters can be calculated or simulated from the guideline outlined in the example. Although  $\pm 10\%$  tolerance on  $Z_{0O}$  is typical and can provide adequate performance, the additional cost of a tighter tolerance results in better channel performance.

## Trace Routing

High-speed serial differential traces are routed with the highest priority to ensure that the optimal path is available to these critical traces. This reduces the need for bends and vias and minimizes the potential for impedance transitions. Traces must be kept straight, short, and with as few layer changes as possible. The impact of vias is discussed in [Differential Vias, page 70](#).

Routing of high-speed traces must be avoided near other traces or other potential sources of noise. Traces on neighboring signal planes should run perpendicular to minimize crosstalk.

Striplines are to be used whenever possible, as are the uppermost and lowermost stripline layers to minimize via stubs. When the stackup is being planned, these layers must be placed as close to the top and bottom layers whenever possible.

Design constraints might require microstrips for the BGA exit path or from via to connector launch or SMT pads. In such cases, the microstrip trace must be kept as short as possible.

Mitered 45-degree bends are recommended (as opposed to 90-degree bends). At a 90-degree bend, the effective width of the trace changes, causing an impedance discontinuity due to the capacitive coupling of the additional conductor area to the reference plane.

The two traces of a differential pair must be length-matched to eliminate skew. Skew creates mismatches in the common mode and reduces the differential voltage swing as a result.

## Plane Splits

Ground planes should be used as reference planes for signals, as opposed to noisier power planes. Each reference plane should be contiguous for the length of the trace, because routing over plane splits creates an impedance discontinuity. In this case, the impedance of the trace changes because its coupling to the reference plane is changed abruptly at the plane split.

## Return Currents

Routing over plane splits also creates issues with the return current. High-speed signals travel near the surface of the trace due to the skin effect mentioned in [Dielectric Losses, page 57](#). Meanwhile, the return current also travels near the surface of the tightly coupled reference plane.

Because of the tight coupling, the return current has the tendency to travel close to the original signal-carrying trace. At the plane split, the return current can no longer follow the same path parallel to the trace, but must instead find an alternative route.

A plane split causes a suboptimal current return path and increases the current loop area, thereby increasing the inductance of the trace at the plane split, changing the impedance of the trace.

## Simulating Lossy Transmission Lines

Due to the different modeling implementations used by various circuit simulators (frequency-domain versus time-domain techniques), it is important to check that the models accurately reflect actual losses. One method is to compare the models against known published configurations.

## Cable

Cables are controlled-impedance transmission lines due to the constant physical dimensions of conductor and dielectric along the length of the cable. The highest quality cable shows little variation in these dimensions and also has a wide bandwidth with low loss at high frequencies.

## Connectors

The connectors attached to cables should exhibit low parasitic inductance, low-parasitic capacitance, and low crosstalk for high bandwidth operation.

## Skew Between Conductors

When selecting a cable, look for a specification of the skew between the conductors in a cable. If the conductors are not length matched, the skew appears in the common mode and directly reduces the eye height.

# Design of Transitions for High-Speed Signals

---

Each transition in the channel must be designed to minimize any negative impact on the link performance. This chapter addresses the interface at either end of a transmission line.

Transmission lines have defined and controlled characteristic impedance along their length. However, the three-dimensional structures that they interface do not have easily defined or constant impedance along the signal path. Software tools such as 3D field solvers are necessary for computing the impedance that a 10 Gb/s signal sees as it passes through these structures, while 2D field solvers are sufficient for computing transmission line characteristic impedance.

PCB designers can use the analyses and examples in this chapter to assist the design of such a channel. Cases not covered in this chapter might need further simulation and analysis.

## Excess Capacitance and Inductance

Most differential transitions are overly capacitive. The P and N paths couple to each other, increasing capacitance. Many transitions have a frequency response identical to that of a lumped capacitor over a wide frequency band.

By design, adding inductance cancels this excess capacitance in many cases except when impacted by density concerns and physical limitations. While techniques such as blind vias, solder balls on a larger pitch, and very small via pads reduce capacitance, they are not always feasible in a design.

Time domain reflectometry (TDR) techniques, either through simulation or measurement, allow the designer to identify excess capacitance or excess inductance in a transition.

## Time Domain Reflectometry

To make TDR measurements, a step input is applied to the interconnect. The location and magnitude of the excess capacitance or inductance that the voltage step experiences as it traverses the interconnect can be determined through observing the reflected signal.

A shunt capacitance (see [Figure 5-1](#)) causes a momentary dip in the impedance, while a series inductance (see [Figure 5-2](#)) causes an impedance discontinuity in the opposite direction.  $T_d$  is the propagation delay through the first transmission line segment on the left. The reflected wave due to the impedance discontinuity takes  $2 * T_d$  to return to the TDR port. If the signal propagation speed through the transmission line is known, the location of the excess capacitance or inductance along the channel can be calculated.

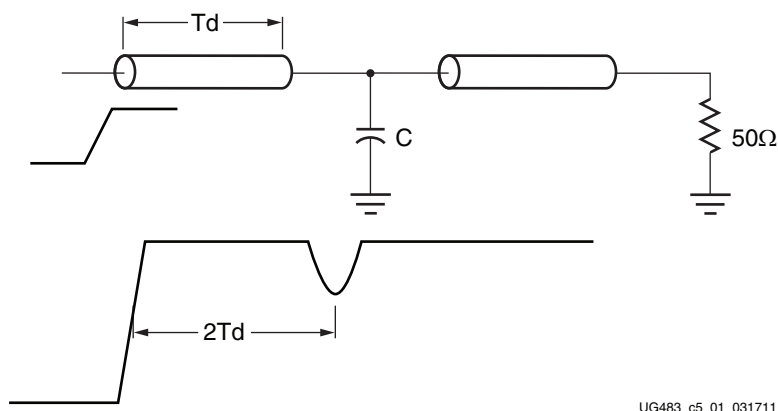


Figure 5-1: TDR Signature of Shunt Capacitance

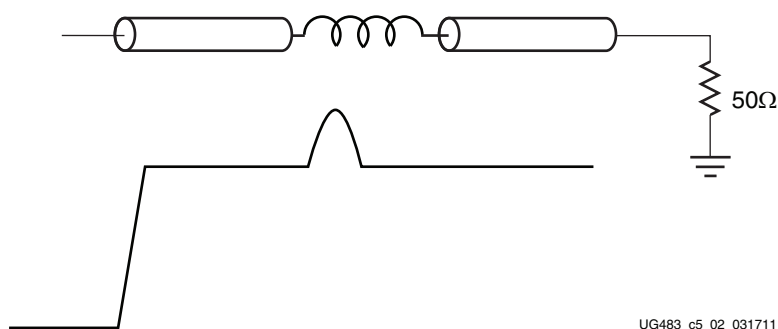


Figure 5-2: TDR Signature of Series Inductance

The magnitude of this excess capacitance (C) or inductance (L) can also be extracted from the TDR waveform by integrating the normalized area of the transition's TDR response. The respective equations for capacitance and inductance are:

$$C = -\frac{2}{Z_0} \int_{t_1}^{t_2} \frac{V_{\text{tdr}}(t) - V_{\text{step}}}{V_{\text{step}}} dt \quad \text{Equation 5-1}$$

$$L = 2Z_0 \int_{t_1}^{t_2} \frac{V_{\text{tdr}}(t) - V_{\text{step}}}{V_{\text{step}}} dt \quad \text{Equation 5-2}$$

Figure 5-3 shows the integration of the normalized TDR area.



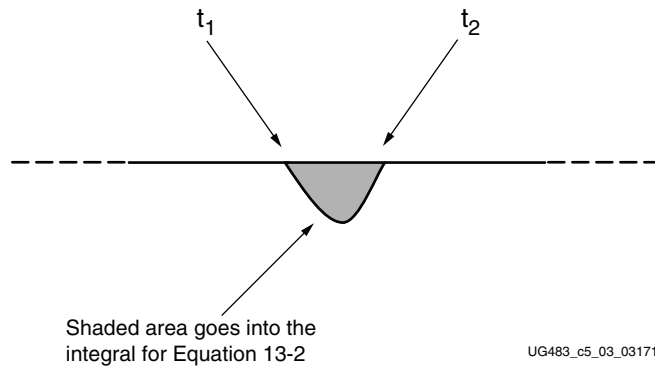


**Figure 5-3: Integration of Normalized TDR Area**

The results using these equations are not sensitive to rise time variation and are valid for simulated TDR measurements provided that the leading and trailing transmission lines are very close to  $50\Omega$ . However, for actual measurements, accuracy is very dependent on  $Z_0$ .

## BGA Package

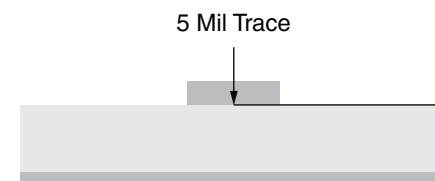
Each signal path within the BGA package is carefully designed to optimize signal integrity. Traces supporting single-ended I/O are nominally designed for  $50\Omega$  trace impedance. Traces supporting high-speed SERDES I/O are designed for nominally  $100\Omega$  differential impedance. Special care is taken in the design of signal paths to optimize discontinuities such as solder balls and substrate vias to minimize their effect on signal integrity. A 3D full-wave electromagnetic solver and a vector network analyzer are used to model and measure package performance.

## SMT Pads

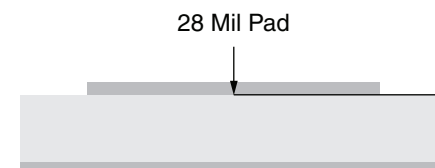
For applications that require AC coupling between transmitter and receiver, SMT pads are introduced in the channel to allow coupling capacitors to be mounted. Standard SMT pads have excess capacitance due to plate capacitance to a nearby reference plane. In the [Figure 5-4](#) example, a 5 mil trace with a  $Z_0$  of  $50\Omega$  transitions to an 0402 SMT pad that is 28 mils wide, all over 3 mils of FR4.

**Line**

- 5.2 mils wide over 3 mil FR4 Dielectric
- $L = 288 \text{ nH/m}$
- $C = 116 \text{ pF/m}$
- $Z_0 = 50\Omega$

**Pad**

- 28 mils wide over 3 mil FR4
- $L = 98 \text{ nH/m}$
- $C = 404 \text{ pF/m}$
- $Z_0 = 16\Omega$



UG483\_c5\_04\_031711

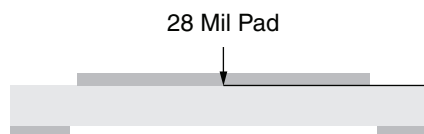
**Figure 5-4: 2D Field-Solver Analysis of 5 Mil Trace and 28 Mil Pad**

Using a 2D field solver on these dimensions yields a  $Z_0$  of  $50\Omega$  for the 5 mil trace. The  $Z_0$  for the 0402 pad is  $16\Omega$  because the pad has too much capacitance and too little inductance, resulting in an impedance of less than  $50\Omega$ . Performance of this transition can be optimized in one of two ways.

The first method makes the trace the same width as the pad and moves the ground plane deeper into the stackup to maintain the  $Z_0$  of the transition at  $50\Omega$ . This method does not require any special analysis, but there might be some error due to the fringing capacitance of the SMT capacitor body. Trace density is limited because traces are now 28 mils wide.

The second method, shown in [Figure 5-5](#), clears the ground plane underneath the pad, which removes much of the excess capacitance caused by the plate capacitance between the pad and the ground plane. This technique allows for greater trace density than the first method, but requires 3D field-solver analysis or measurement along with several board iterations to get the desired performance.

- $L = 241 \text{ nH/m}$
- $C = 89 \text{ pF/m}$
- $Z_0 = 52\Omega$

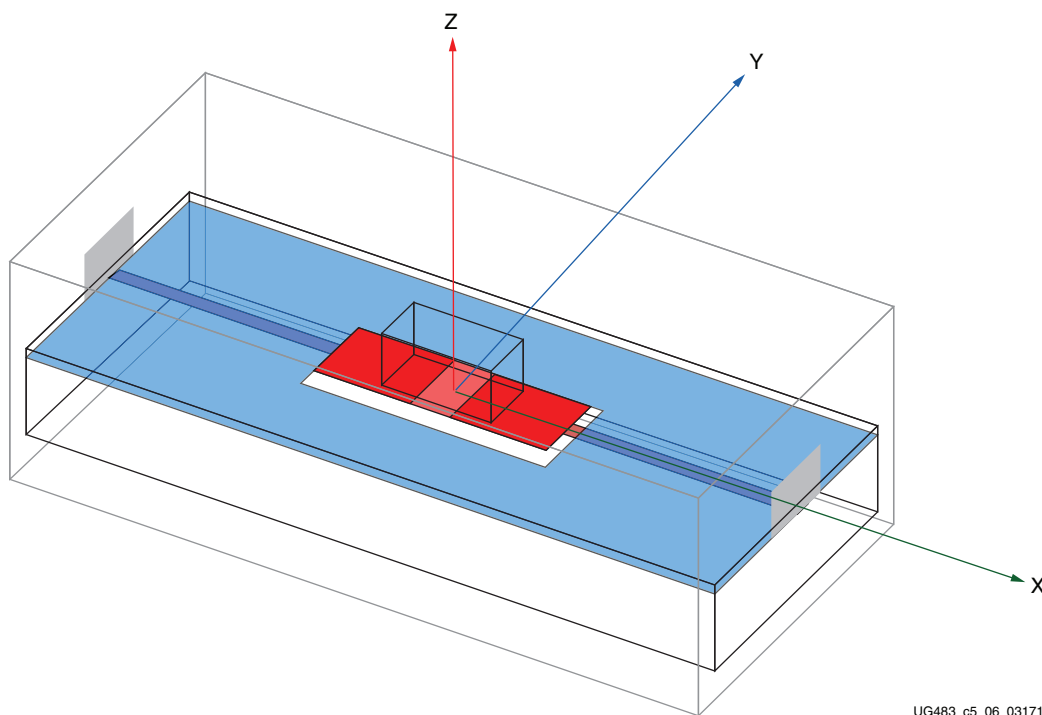


UG483\_c5\_05\_031711

**Figure 5-5: Transition Optimization**

The 2D field-solver example shows that close to  $50\Omega$  can be achieved if the ground plane under the pad footprint is cleared out. A 3D field solver is then used to verify this result to a greater degree of accuracy.

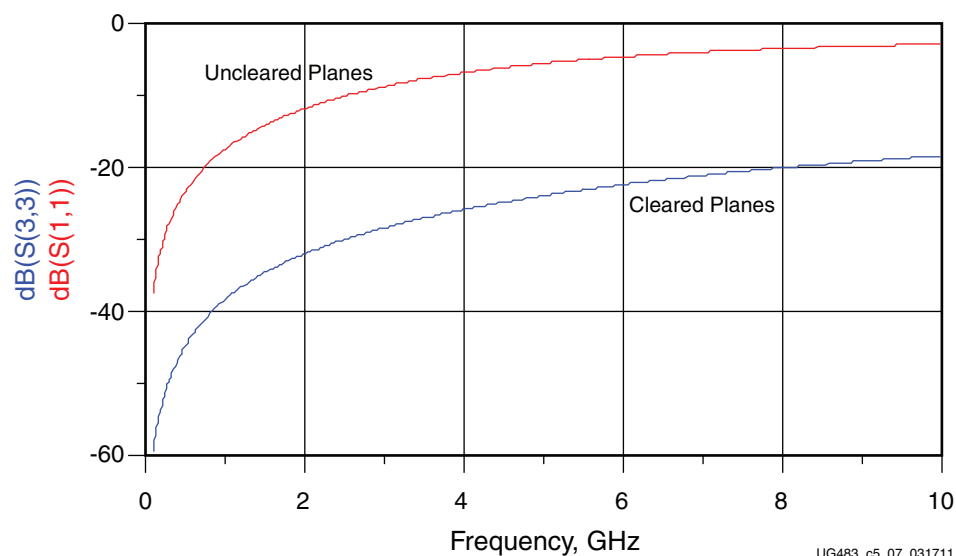
[Figure 5-6](#) shows the ground plane cleared away exactly as it was for the 2D simulation. Using frequency domain analysis within HFSS, there is a 20 dB (10x) improvement in return loss using this technique.



UG483\_c5\_06\_031711

**Figure 5-6: Ansoft HFSS Model of Pad Clear-Out**

Figure 5-7 shows the return loss comparison between 0402 pad structures with linear scale.



UG483\_c5\_07\_031711

**Figure 5-7: Return Loss Comparison Between 0402 Pad Structures**

The approximately  $-40$  dB/decade slope in Figure 5-8 shows good fit to the frequency response of a lumped capacitor.

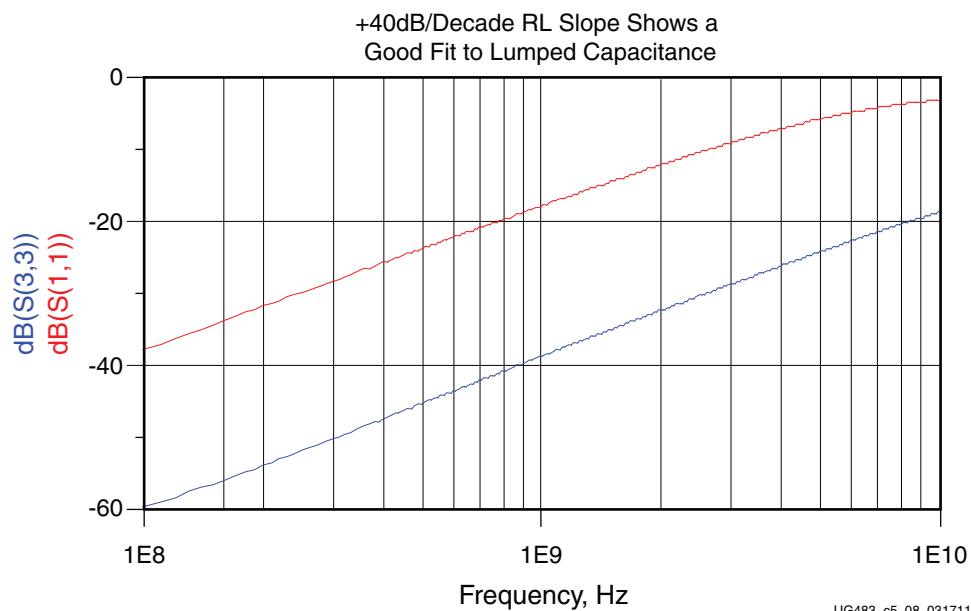


**Figure 5-8: Return Loss Comparison Between 0402 Pad Structures on Log (Frequency) Scale**

Next, using simulated measurements on the same transition modeled in HFSS, the time-domain performance of this transition can be measured by doing a TDR on the S-parameter results from the earlier frequency domain analysis.

In [Figure 5-9](#) and [Figure 5-10](#), the red curve with the large capacitive dip corresponds to the SMT pad without the ground plane cleared from underneath. The blue curve shows that clearing out the ground plane removes much of the excess capacitance. This improvement can be quantified using [Equation 5-1](#) and [Equation 5-2](#).

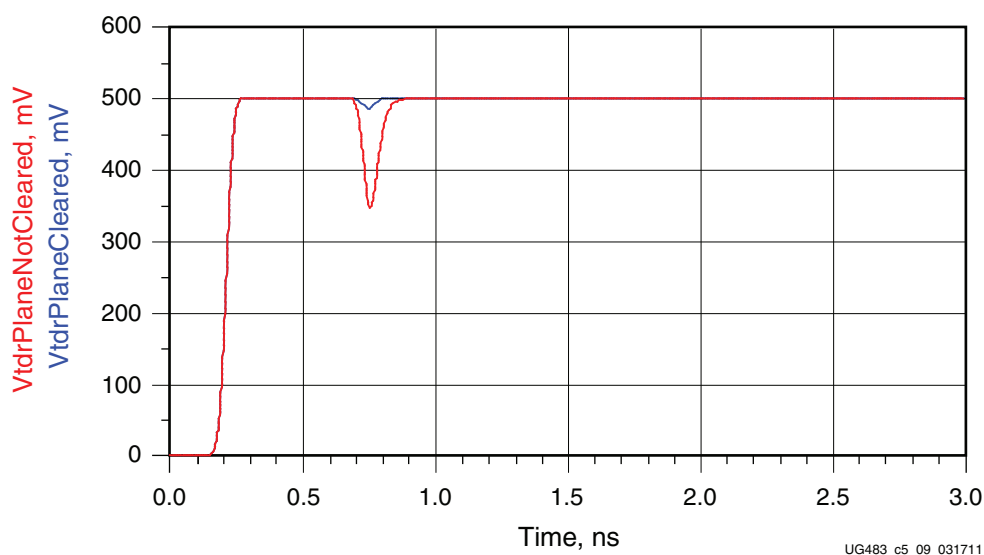


**Figure 5-9: TDR Results Comparing 0402 Pad Structures**

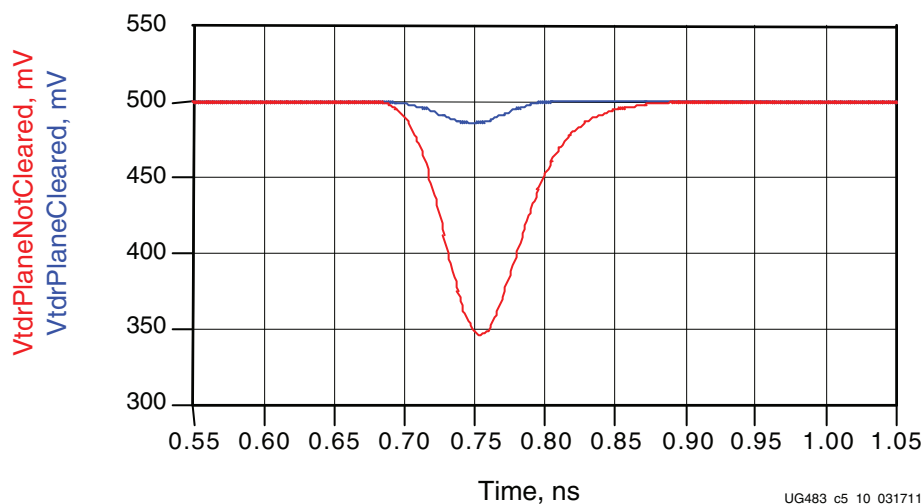


Figure 5-10: TDR Results Comparing 0402 Pad Structures

As shown from Figure 5-11 and Figure 5-12, clearing the ground plane under SMT pads yields a significant improvement in the performance of an SMT pad transition. Excess capacitance is reduced by 15x, and return loss is improved by 20 dB.

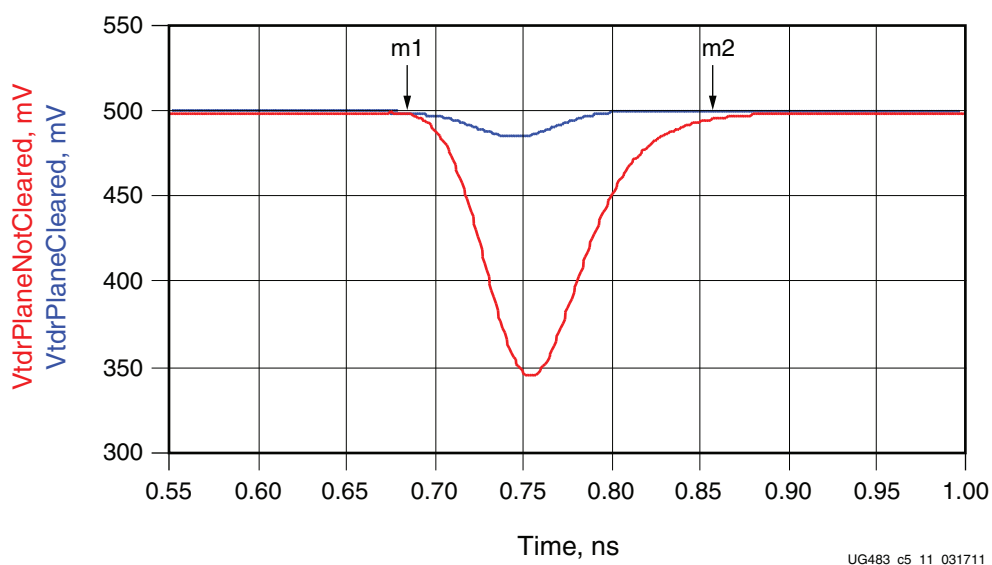


Figure 5-11: 840 fF Excess Capacitance with Ground Plane Intact

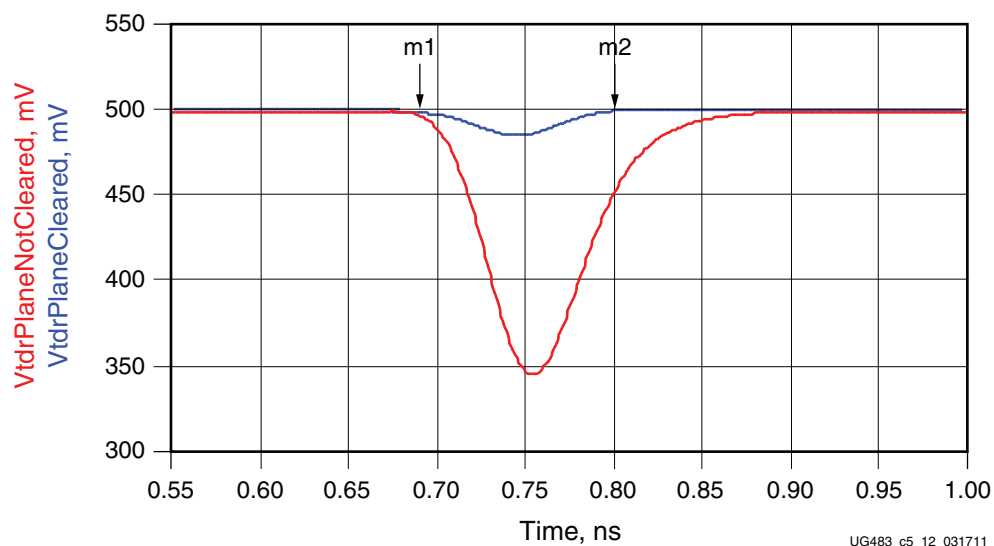


Figure 5-12: 57 fF Excess Capacitance with Ground Plane Intact

## Differential Vias

The most common transition is the differential via where the signal pair must transition from an upper stripline layer or top microstrip to a lower stripline layer or bottom microstrip.

Figure 5-13 shows a Ground-Signal-Signal-Ground (GSSG) type differential via. Ground vias are connected to each ground plane in the stackup, while signal layers only contain pads for the entry and exit layers.

Via Diameter = 12 mils (0.012 inches)  
 Pad Diameter = 22 mils  
 Annular Ring = 5 mils  
 GSSG Via Pitch = 40 mils  
 Oblong Antipads = ~55 mils x 95 mils,  
 aligned with ground pads

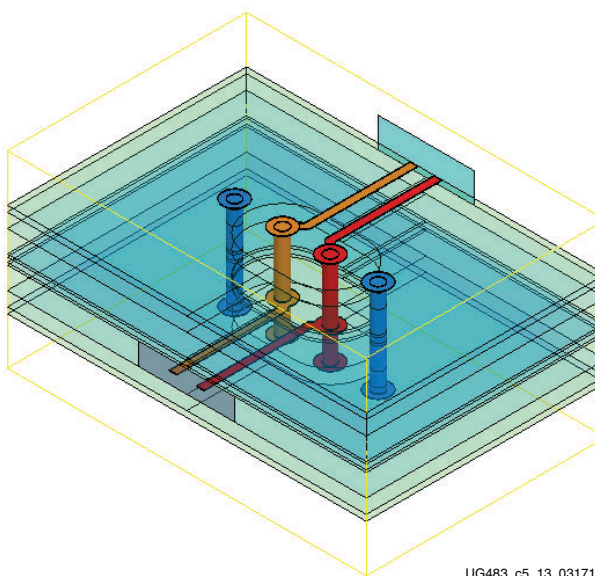


Figure 5-13: Differential Via Design Example

A key advantage of a GSSG via is that it allows for the signal's return current to flow in the ground via near the corresponding signal via, reducing excess inductance. The signal path is also symmetrical between the P and N halves of the differential signal, which is critical in controlling common-mode artifacts due to P/N imbalance.

The larger oblong antipads reduce excess fringing capacitance between the via body and the surrounding planes edges. Unused pads are also removed.

A good starting point is to use the dimensions shown in Figure 5-13 as an example differential via design for an 80 mil board. To accommodate density constraints or the lack thereof, the dimensions can be scaled accordingly to preserve the ratios of each dimension relative to the others. Such scaling preserves the impedance performance of the differential via while allowing variation in overall size to better suit specific applications. These final dimensions are limited by manufacturability and density constraints.

While the via length can be varied by a small amount to suit boards that are thicker or thinner than the 80 mil example, changing the ratio of the via length relative to other dimensions affects the via's impedance. For this and other configurations of differential vias, it is best to simulate a model using 3D field-solver tools to ensure that performance targets are met.

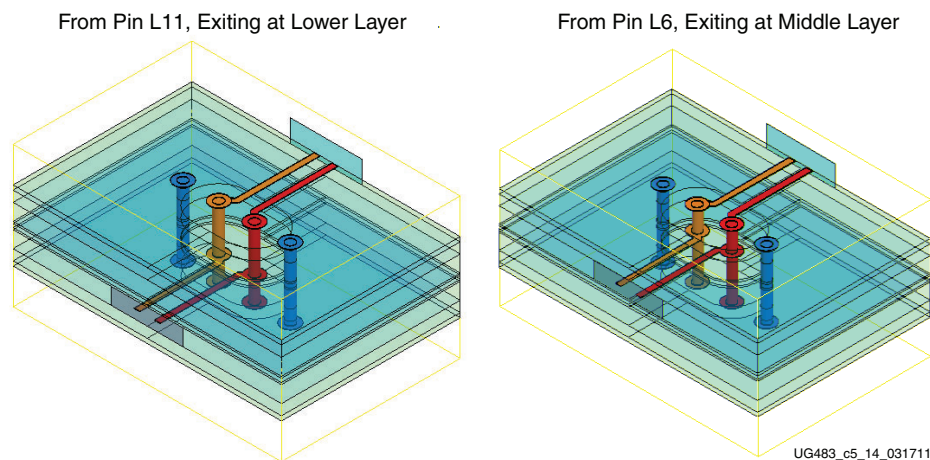


**Figure 5-14: Differential GSSG Via in 16-Layer PCB from Pins L11 and L6**

As a general rule, the P and N paths need to be kept at equal lengths through a transition. Where possible, via stub length should be kept to a minimum by traversing the signal through the entire length of the vias. The analysis shown in Figure 5-15 compares the S-parameter return loss for common-mode (SCC11) and differential (SDD11) responses.

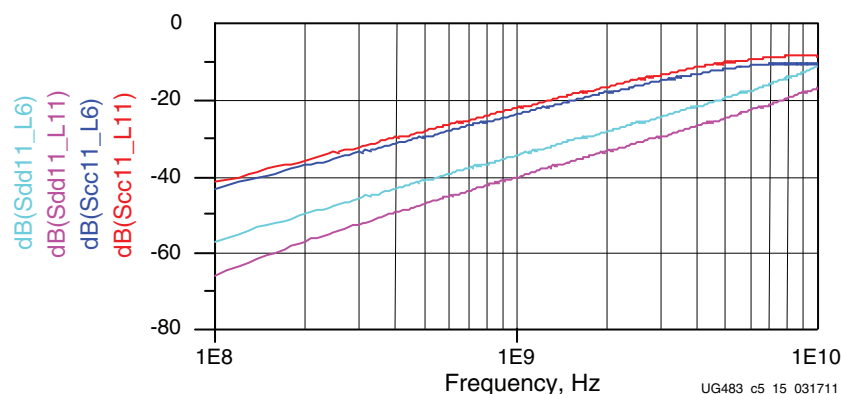


**Figure 5-15: Simulated Return Loss Comparing Differential and Common-Mode Losses for L11 and L6 GSSG Vias**

From the graph in [Figure 5-15](#), the common-mode response is 20 dB worse in terms of return loss. The much worse common-mode response relative to the differential response is the reason why it is a good idea to reduce P/N skew as much as possible before entering a transition. The 60/40 rule of thumb is 40 dB of return loss at 1 GHz, which implies 60 fF of excess capacitance. Because excess capacitance is a single pole response, simple extrapolation rules can be used. For example, a shift to 34 dB return loss doubles the excess capacitance. Due to the excellent performance characteristics of GSSG vias, even long via stubs only double the differential via's capacitance at the most.



## P/N Crossover Vias

Some transceivers offer the ability to independently switch the polarity of the transmit and receive signal pairs. This functionality eliminates the need to cross over the P/N signals at the board level, which in turn significantly enhances signal integrity. If possible, P/N crossover vias are to be avoided and the polarity switch of the transceiver should be used.

## SMA Connectors

Well-designed SMA connectors can reduce debugging time and allow a high-performance channel to be designed correctly on the first pass. SMA connectors that perform well at 10 Gb/s need to be simulated, designed, and manufactured to meet this performance target. Vendors can also offer design services that ensure that the connector works well on a specific board. Assembly guidelines are crucial in ensuring that the process of mating the connector to the board is well-controlled to give the specified performance.

Xilinx uses precision SMA connectors from Rosenberger and other precision connector manufacturers because of their excellent performance and because of the points listed in the previous paragraph.

## Backplane Connectors

There are numerous signal integrity issues associated with backplane connectors including:

- P/N signal skew
- Crosstalk
- Stubs due to connector pins

Some connector manufacturers offer not only S parameters, models, and layout guidelines for their connectors but also design support, seminars, and tutorials.

## Microstrip/Stripline Bends

A bend in a PCB trace is a transition. When routing differential traces through a 90° corner, the outer trace is longer than the inner trace, which introduces P/N imbalance. Even within a single trace, signal current has the tendency to hug the inside track of a corner, further reducing the actual delay through a bend.

To minimize skew between the P and N paths, 90° turns in microstrips or striplines are routed as two 45° bends to give mitered corners. The addition of a jog-out also allows the trace lengths to be matched. [Figure 5-16](#) shows example bends in traces.

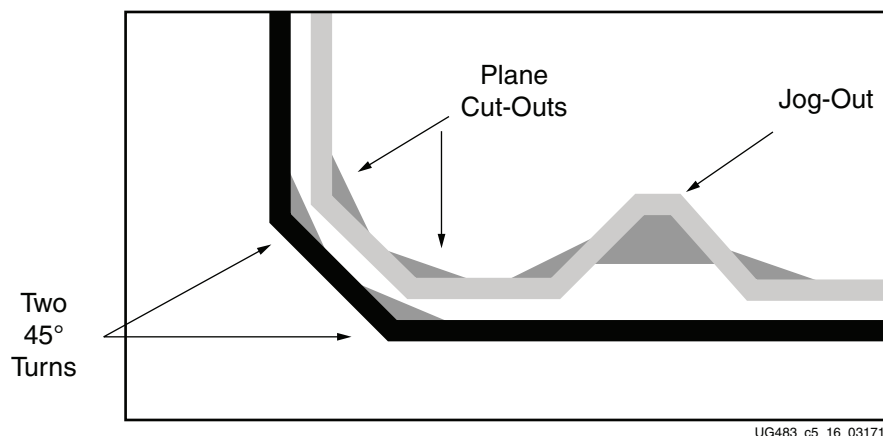


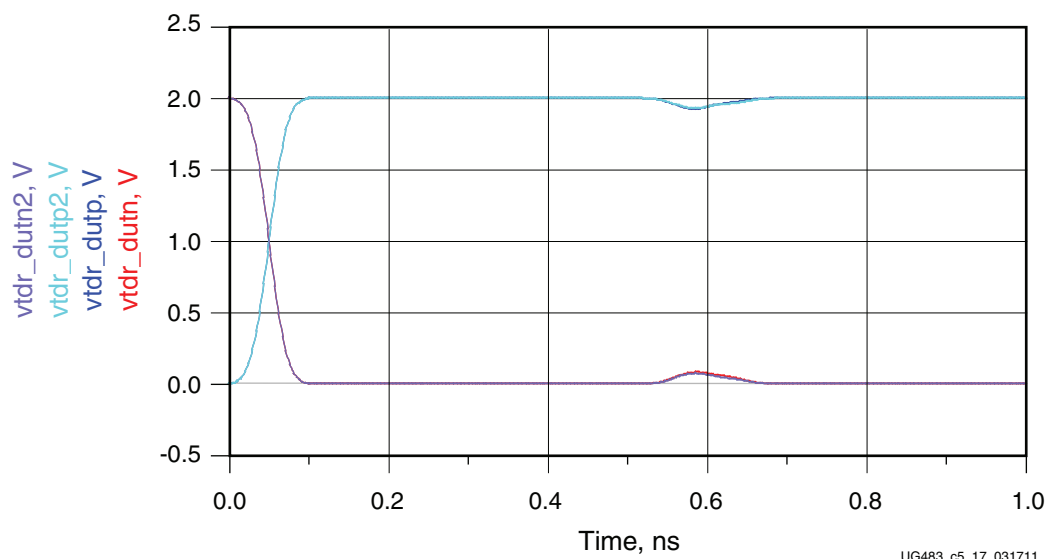
**Figure 5-16: Example Design for 90 Degree Bends in Traces**

Turns add capacitance because the trace at a 90° corner is 41% wider. That difference is reduced to 8% with a 45° turn. The addition of plane cutouts to a depth of 30 mils act to reduce this amount of excess capacitance. The trace was not widened to maintain 50Ω with the plane cutouts in place.

When this mitered bend is simulated with the jog-out and plane cutouts, excess capacitance is reduced and P/N length and phase matching is improved. Without jog-outs, the P/N length mismatch is 16 mils. Given FR4 material, the 16 mil difference translates to a phase mismatch of 4.8° at 5 GHz, or 2.68 ps (0.0268 UI) at 10 Gb/s.

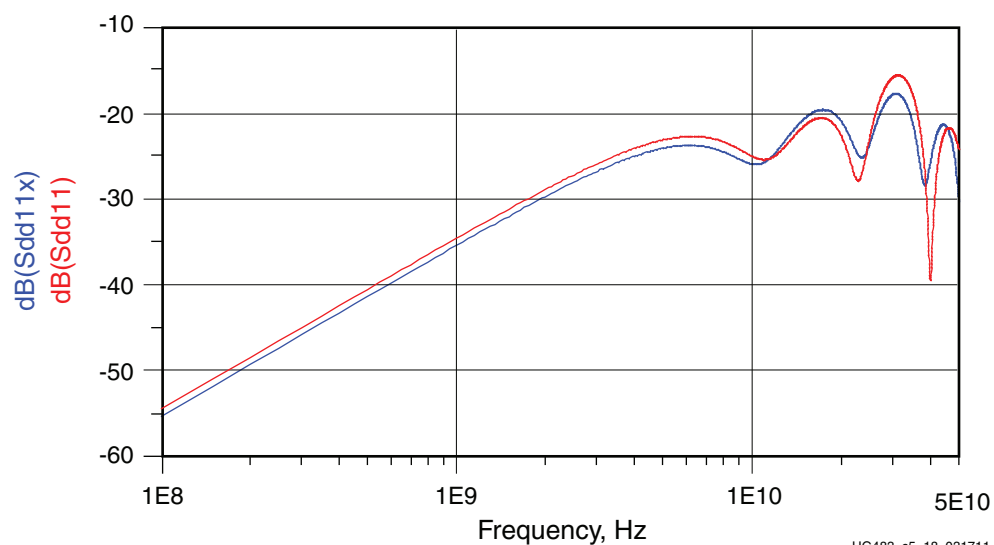
Figure 5-17 through Figure 5-19 show that phase mismatch is reduced to 0.75° with jog-outs and 0.3° with jog-outs and plane cutouts. The combination of jog-outs and plane cutouts yields simulation results that show the excess capacitance of the structure is reduced to 65 fF.

Designers are tempted to widen lines to compensate for the characteristic impedance increase as the lines are separated and couple less strongly. However, even without widening the lines, the combined capacitance of the corners and jog-outs is still overly capacitive, and therefore the uncoupled section of the jog-out must not be widened.



UG483\_c5\_17\_031711

Figure 5-17: Simulated TDR of 45 Degree Bends with Jog-Outs



UG483\_c5\_18\_031711

Figure 5-18: Simulated Return Loss of 45 Degree Bends with Jog-Outs

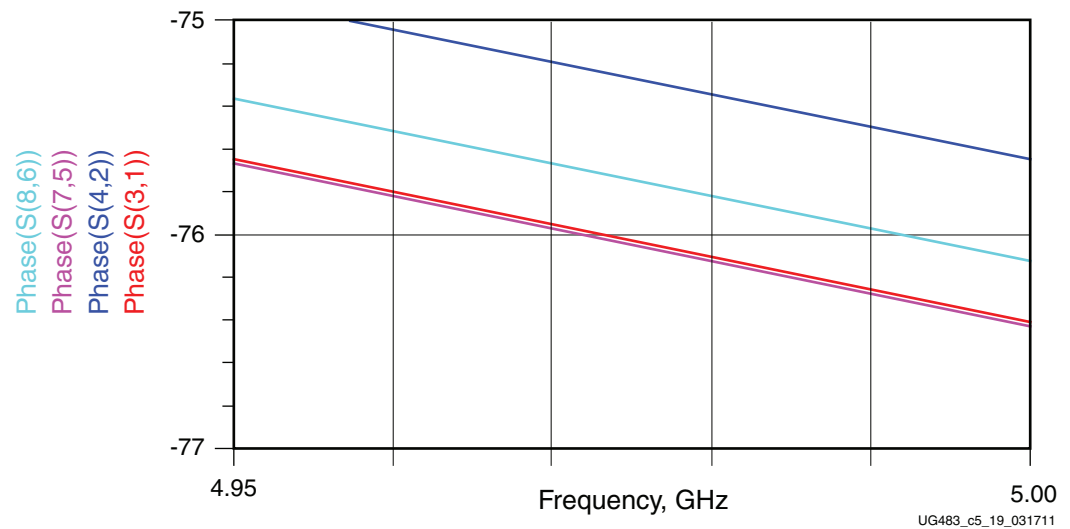


Figure 5-19: Simulated Phase Response of 45 Degree Bends with Jog-Outs

For wide traces, curved routing can also be helpful as shown in Figure 5-20.

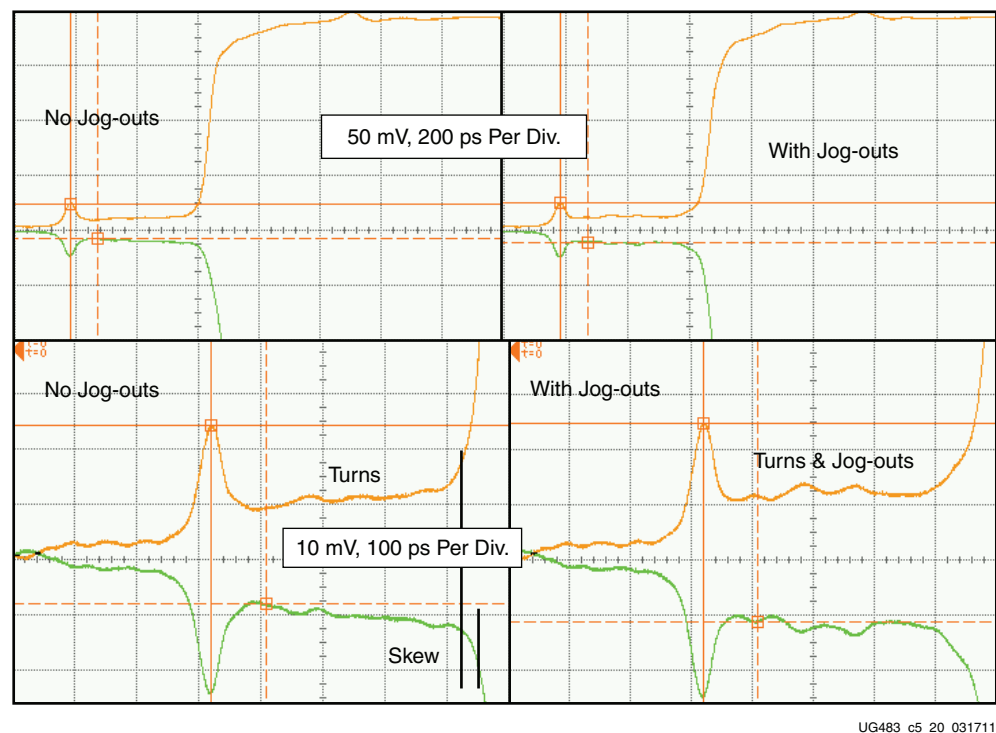


Figure 5-20: Measured TDR of 45 Degree Bends with and without Jog-Outs